

“Every sentence I utter must be understood not as an affirmation, but as a question.”

~N. H. D. Bohr

University of Alberta

**Catalytic cracking and upgrading of oilsands bitumen using
natural calcium chabazite**

by

Christopher Alan Street

A thesis submitted to the Faculty of Graduate Studies and Research
in partial fulfillment of the requirements for the degree of

Master of Science

in

Chemical Engineering

Department of Chemical and Materials Engineering

©Christopher A. Street

Fall 2011

Edmonton, Alberta

Permission is hereby granted to the University of Alberta Libraries to reproduce single copies of this thesis and to lend or sell such copies for private, scholarly or scientific research purposes only. Where the thesis is converted to, or otherwise made available in digital form, the University of Alberta will advise potential users of the thesis of these terms.

The author reserves all other publication and other rights in association with the copyright in the thesis and, except as herein before provided, neither the thesis nor any substantial portion thereof may be printed or otherwise reproduced in any material form whatsoever without the author's prior written permission.

Abstract

The growing interest in the oilsands bitumen reserves, a large portion of which is unattainable by current industrial processes, has generated a need for an improved process for oilsands extracting and upgrading.

The effects of using chabazite as a catalyst for cracking and upgrading of oilsands bitumen were studied. At 300 °C and 5 % catalyst loading the yield of the desirable middle fractions was maximized while avoiding overcracking that produces gas and coke. The natural zeolite also upgraded the bitumen as it was being cracked and greatly reduced the amount of water used.

An energy balance comparison between the current industrial method and our proposed process, and tests on pre-extracted bitumen, show that a zeolite based upgrading process is more energy efficient. The reported method has great potential for improving the *in situ* extraction methods, reducing their startup time and upgrading the bitumen while it is being extracted.

I would like to acknowledge those who helped me, from first starting in the lab and piquing my interest in research, to turning this jumble of ideas into a coherent and legible thesis.

Dr. S.M. Kuznicki, for starting me on the path and supporting me throughout.

C.C.H. Lin, for inspiring me and showing me how far hard work and dedication can take you.

W. An, W. Wei, S. Zhou, M. Rahman, J. Kim and all the people in the lab who helped me with the research work.

A.S.M. Junaid, for the guidance during the research, reviewing my thesis and the Timbits throughout.

A. Zeko, for putting the final polish on my thesis.

To my friends who made this such a wonderful adventure, to Terri for always supporting me and walking all the way to my office, and finally my family, for the support: financial, emotional and nutritional.

Table of Contents

Chapter One. Introduction	1
1.1 What Is Bitumen	1
1.2 Current Harvesting Techniques	3
1.2.1 Mining Techniques	4
1.2.2 <i>In situ</i> Techniques	5
1.3 Zeolites	7
1.3.1 Zeolite Framework	7
1.3.2 Zeolites' Cracking Ability	9
1.4 Catalytic Cracking Using Natural Zeolites	11
1.4.1 Proof of Concept Studies Using Microreactors	11
1.4.2 Stirred Reactions	12
Chapter Two. Experimental	14
2.1 Materials	14
2.1.1 Feed Components	14
2.1.2 Catalyst and Control Material	15
2.1.3 Catalyst Characterization	15
2.1.4 Dean Stark Analysis	16
2.2 Reactions	18
2.2.1 Stirred Oilsands Reactions	18

2.2.2 Bitumen Reactions	23
2.3 Extraction	26
2.4 Coke	28
2.5 Viscometry	29
2.6 SARA Fractionation	31
Chapter Three. Results and Discussion	36
3.1 Characterization of Materials	36
3.2 Stirred Oilsands Reactions	40
3.2.1 Product Yields	40
3.2.2 Product Quality	48
3.3 Energy Balance	52
3.4 Bitumen Reactions	58
3.5 Error	63
Chapter Four. Conclusion	65
Chapter Five. Bibliography	68
Chapter Six. Appendix	73

List of Tables

Table 1-1.	Breakdown of the total and extractable amount of bitumen by minable and <i>in situ</i> recovery methods in Alberta	2
Table 3-1.	Results of the Dean Stark analysis in weight %	36
Table 3-2.	BET and EDX analysis of calcium chabazite and zeolite Y	38
Table 3-3.	Error percentages of all product yields for the stirred oilsands reactions	49
Table 3-4.	Error percentages of SARA products	54
Table 3-5.	A basic energy balance around the current industrial cracking and extracting process and the proposed natural zeolite process	56
Table 3-6.	A basic energy balance for both the current industrial upgrading process and the proposed zeolitic upgrading process	60

List of Figures

Figure 1-1.	Cross sectional view of the SAGD steam envelope as seen parallel to the two wells.	6
Figure 1-2.	Chabazite structural framework from a [001] orientation Showing the two secondary building units, A) the d6r unit and B) the CHA unit.	8
Figure 1-3.	Structure of the Brønsted acid site in the silica-alumina framework.	9
Figure 2-1.	Dean Stark analysis experimental setup.	17
Figure 2-2.	Diagram of the stirred oilsands reactor.	19
Figure 2-3.	Diagram of the reactor in the heating mantle, PID controller and the mixing apparatus.	21
Figure 2-4.	Shaker assembly with reactor placed in sandbath.	25
Figure 2-5.	Viscometer with the bob and cup inside the heating jacket.	29
Figure 2-6.	Millipore asphaltenes extraction set-up.	31
Figure 2-7.	Column set up for the SARA fractionation test.	33
Figure 3-1.	SEM images of A) Chabazite and B) Zeolite Y	37
Figure 3-2.	XRD patterns of calcium chabazite and zeolite Y	39
Figure 3-3.	Amounts of maltenes recovered from the stirred oilsands reactions.	41

Figure 3-4.	Amount of gas collected from the stirred oilsands reactions.	43
Figure 3-5.	Amount of C5 asphaltenes left after the stirred oilsands reactions.	44
Figure 3-6.	Amount of coke generated by the stirred oilsands reactions	46
Figure 3-7.	Overall reaction product breakdown of the stirred oilsands reactions.	48
Figure 3-8.	SARA fractionation products of the stirred oilsands reactions.	50
Figure 3-9.	Viscosities of the stirred oilsands reactions.	52
Figure 3-10.	The proposed zeolite process and the current industrial process for oilsands bitumen cracking and upgrading.	55
Figure 3-11.	Viscosities of the stirred oilsands reactions.	61
Figure 3-12.	Bitumen product viscosities for thermal and 10 % calcium chabazite catalyst reactions at 300 °C as a function of varying reaction times.	63
Figure 3-13.	Reusability runs with 10 % reactant loading at 300 °C across two runs as a function of viscosity.	65

Nomenclature

ASTM	American society for testing and materials
BET	Brunauer, Emmett and Teller
CC	Calcium chabazite
CHA	Chabazite secondary building unit
CHWE	Clarks hot water extraction
CSS	Cyclic steam stimulation
C#	Paraffinic carbon chain of length #
EDX	Energy dispersive x-ray
FCC	Fluid catalytic cracking
g	Grams
He	Helium
J	Joules
kpa	Kilopascals
L	Litre
L/h	Litres per hour
m	Meters
m ³	Cubed meters
OS	Oilsands
PID	Proportional-integral-derivative

PGT	Princeton gamma-tech
P-Ex	Pentane Extract
REUSY	Rare earth ultra stable zeolite Y
rpm	Rotation per minute
SAGD	Steam assisted gravity drilling
SARA	Saturates aromatics resins asphaltenes
SEM	Scanning electron microscopy
USY	Ultra stable zeolite Y
XRD	X ray diffraction

Chapter 1. Introduction

1.1 What is Bitumen?

Bitumen is one of the heaviest and most viscous forms of the natural crude oil produced by the oil industry. It is extracted from oilsands deposits where anaerobic hydrocarbon-eating bacteria once lived. The bacteria ate the smaller hydrocarbons, leaving behind the larger molecules and longer chains which combined with water washing and physical and chemical weathering turned what could have been a normal oil deposit into the tarry and difficult to handle bitumen known today as oilsands deposits^[1]. Bitumen is defined as “a complex mixture consisting of compounds ranging from nonpolar aliphatic and naphthenic hydrocarbons to highly polar aromatic molecules containing heteroatoms such as oxygen, nitrogen, and sulfur”^[2]. Bitumen also contains transitional metal ions that can be bound in porphyrin rings that further contribute to the poor bitumen quality. Bitumen’s heaviest fraction, the asphaltenes, is responsible for most of the bitumen’s large molecular weight and more importantly, its viscosity. If even a small amount of the asphaltenes can be cracked into smaller fragments, it will greatly improve the bitumen’s viscosity^[3].

The largest oilsands deposits in the world are located in Alberta, accounting for 96% of all the oil in Canada. This boosts Canada’s oil reserves to be the second largest next to Saudi Arabia^[4]. The oilsands, though one of the most abundant

sources of petroleum and in production since 1967, have only recently become an area of major development. With the increasing price of oil, the harvesting of oilsands, despite its methods being quite expensive, is becoming more popular. For example, production of mined bitumen has tripled since 1990, while the production of *in situ* bitumen has grown more than 5 times^[5]. Table 1-1 shows the total amount of bitumen (initial volume in place), the amount of that bitumen that is able to be harvested with current technology (initial established reserves) and a breakdown of those established reserves.

Table 1-1 – Breakdown of the total and extractable amount of bitumen by minable and *in situ* recovery methods in Alberta in 2009 (values are $\times 10^9 \text{ m}^3$)

Reproduced with permission^[6]

Recovery method	Initial volume in place	Initial established reserves	Cumulative production	Remaining established reserves	Remaining established reserves under active development
Mineable	20.8	6.16	0.72	5.44	3.69
In situ	<u>265.8</u>	<u>21.94</u>	<u>0.38</u>	<u>21.55</u>	<u>0.53</u>
Total	286.6 (1 804) ^b	28.09 ^a (176.8) ^b	1.10 (6.9) ^b	26.99 (169.9) ^b	4.22 (26.5) ^b

^a Differences are due to rounding.

^b Imperial equivalent in billions of barrels.

It is easy to see why the *in situ* production has grown so much compared to the more easily accessed mineable sands. By subtracting the reserves under active development from the remaining established reserves, it can be seen that the

mining operations have only $1.75 * 10^9 \text{ m}^3$ of crude bitumen not under current development. There is much more room for growth in the *in situ* development, an order of magnitude more, with $21 * 10^9 \text{ m}^3$ of undeveloped crude bitumen. Another interesting figure is that 30% of the volume of total bitumen in the mineable section is currently extractable and an even smaller amount, 8%, of the *in situ* bitumen. This leaves a large window of opportunity for the development of new methods to increase the amount of bitumen which may be harvested. This opportunity is also shown by some sources, which estimate that the oilsands production levels in 2016 are expected to triple the 2006 levels ^[7], making the technological development of superior oilsands practices an important and worthwhile endeavor.

1.2 Current Harvesting Techniques

The oilsands are made of deposits that are mineable and ones that require *in situ* operations in order to extract the bitumen. The minable areas are deposits that can be dug out, collecting the oilsands with large-scale operations that involve massive machines. In 2009, Alberta processed approximately 1.5 million tons per day using these mining methods ^[5]. The payzones that can be economically extracted by mining operations are generally less than 50 m deep (to the top of the payzone), with a thickness of at least 3 m ^[8]. This is currently the most popular method of extraction as seen in Table 1, where 87 % of the active development is in the mineable areas. The areas too deep for mining operations must be harvested by *in situ* methods. Wells can be drilled down to the deposit but the

bitumen is very viscous, so much so that it does not flow at normal temperatures. This has forced the oilsands industry to develop techniques to improve the viscosity of bitumen while *in situ*, which makes the process much more difficult.

1.2.1 Mining Techniques

Currently the process used to extract the bitumen from the mineable oilsands deposits is the Clark Hot Water Extraction (CHWE) process. This process is undergoing continuing improvements. One significant improvement was the switch from conveyor belts to a hydrotransport process that separates the bitumen from the sand during transport. Another improvement was a reduction in the temperature of the process, from 75 °C to 50 °C, with a proposed process going as low as 25 °C^[9]. After the hydrotransport, the liberated bitumen and sand are separated in a gravity separation vessel. This is the main extraction step where the majority of the sand and water are separated from the bitumen stream. The liberated oil droplets attach to air bubbles and float to the top of the vessel, while the heavy sand and water are taken out of the bottom. The froth on top is taken off and deaerated using steam, after which it proceeds to froth treatment to get rid of the remaining sand and water.

There are two common froth treatment processes: naphthenic and paraffinic treatment. In both processes the froth is combined with a diluent, then a combination of settlers and/or centrifuges are used in series to remove the sand and water from the bitumen. Some key differences exist between the two processes other than their namesake solvents. The paraffinic treatment is

conducted at a lower temperature (30 °C) than the naphthenic treatment at 75 °C but it has a higher solvent to bitumen ratio than the naphthenic treatment (2.3 vs. 0.7). Additionally, the paraffinic treatment produces a higher quality bitumen, with a water concentration of 0.2 % and a solid concentration of 0.01% compared to the naphthenic process (3 % and 0.5 % respectively). Finally during the paraffinic process some of the asphaltenes are lost in the tailings stream due to precipitation, 50 % of the asphaltenes, giving the naphthenic treatment an advantage with a better bitumen recovery percentage ^[10].

1.2.2 *In situ* Techniques

Two of the most common types of *in situ* harvesting methods are SAGD (Steam Assisted Gravity Drilling) and CSS (Cyclic Steam Stimulation), although there are many others in various stages of development. The most common method, first put into production in 2001, is SAGD. In this process two horizontal wells are drilled one on top of each other, 5 m apart. The top wellbore is used to inject steam into the reservoir which heats up the bitumen surrounding it until it becomes fluid enough to flow to the bottom well where it can be taken out. The following figure illustrates the steam chamber and how it continues to expand, Figure 1-1.

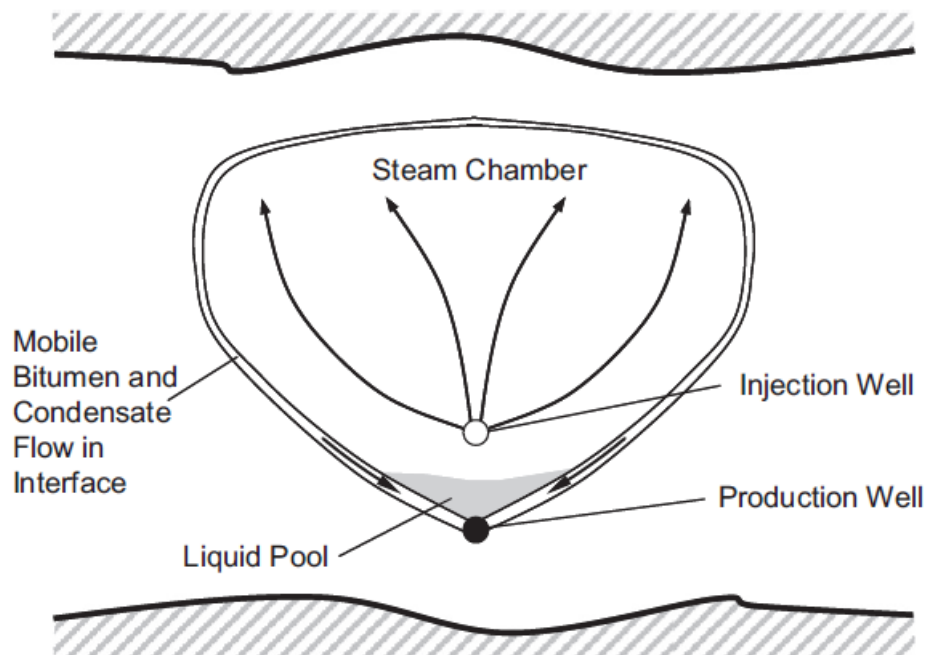


Figure 1-1 – Cross sectional view of the SAGD steam envelope as seen parallel to the 2 wells. Reproduced with permission ^[11].

SAGD is particularly effective because the injected steam rises and heats up the oil above it and the heated oil flows down into the producing well, which is then brought to the surface ^[12]. This forms the steam chamber, which continues to grow upward, heating more oil to be harvested in the bottom production well.

The main operational problem with bitumen is its viscosity. Not only does it create difficulties getting the bitumen out of the ground in *in situ* operations but it also causes transport and handling problems in the processes following extraction in both *in situ* and mining operations ^[13]. To counter this, different methods must be used to keep the bitumen flowing with heating being used in plants or diluents

for pipeline transport. Diluents have become popular due to the low amount required, but their use adds to the cost and complexity of the operation ^[14]. Any novel approaches to upgrading the bitumen earlier in the extraction process would save on future upgrading steps and simplify transporting and harvesting issues.

1.3 Zeolites

Zeolites are a common, inexpensive mineral that can be found all over the world. The useful properties of zeolite are myriad and can be classified into three main types of use, namely, acting as adsorbents, used as molecular sieves and catalytic cracking. Specifically in the petroleum industry, zeolite started to be used as a catalyst in 1959 when Union Carbide used zeolite Y as an isomerization catalyst for petroleum cracking ^[15]. Currently in industry, zeolites are mainly used for Fluid Catalytic Cracking (FCC), but also aid in many other catalytic petrochemical processes.

1.3.1 Zeolite framework

Zeolites are crystalline minerals with a unique framework and composition that give them very useful properties. The framework is composed of $[\text{SiO}_4]^{4-}$ and $[\text{AlO}_4]^{5-}$ that form a repeating crystal structure of pores, each the exact same size, creating a series of channels through the crystal ^[15]. Figure 1-2 reveals the unit cells that build the chabazite crystal lattice structure.

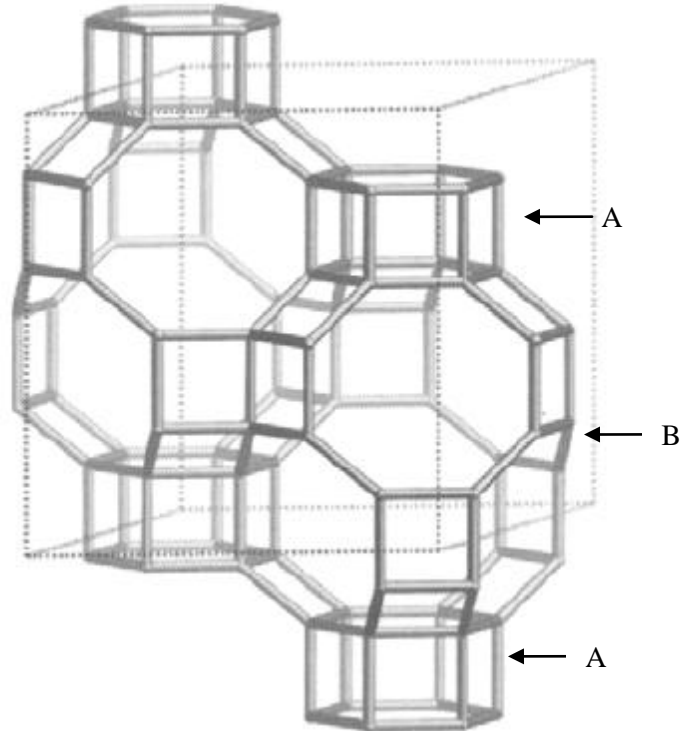


Figure 1-2 – Chabazite structural framework from a [001] orientation showing the two secondary building units, A) the d6r unit and B) the CHA unit.

Reproduced with permission ^[16]

The two unit cells are orientated normal to the [001] crystallographic plane and it can be seen that each unit cell is comprised of two secondary building units: the d6r, which is the short hexagonal cylinder on top and the bottom of the crystal unit. The other unit is the CHA building unit ^[16]. The CHA building unit is not specific solely to chabazite but can be found in many other types of zeolite, though chabazite is by far the most commonly occurring zeolite with this framework. The pores that pass through the zeolite can be seen as the channel,

formed by the 8 membered rings, that progress at a downward 45 degree angle from the viewpoint in Figure 1-2.

1.3.2 Zeolites' Cracking Ability

Zeolites owe their cracking ability to the acid sites attached to aluminum in their framework. These sites are Brønsted acid sites located on the bridging hydroxyl group that are connected to the framework aluminum^[17]. Due to the tetrahedral Si being bonded to a tri-coordinated Al through O, the Al has a negative charge. The negative charge is usually balanced by a metal ion but when exchanged with hydrogen, acts as a Brønsted acid site. Figure 1-3 shows the hydroxyl group in between the silica and aluminum framework atoms.

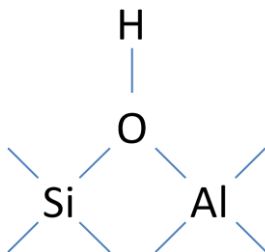


Figure 1-3 – Structure of the Brønsted acid site in the silica-alumina framework.

Many theoretical studies were done to understand the behavior of the acid sites, some even using quantum mechanics to determine the exact location and energies

involved in the site interaction. Due to the small size of zeolite pores, the bitumen molecules, especially the large asphaltenes, can only react on the exterior surface of the zeolite ^[18].

Zeolites are used in many different refining and upgrading processes, such as isomerization, hydrocracking and dewaxing. Many of these involve the cracking of heavier, longer molecules into smaller, more valuable products. An important property of the zeolites is their crystallographic unit cell size. The cell size is a rough measure of the Si/Al ratio, which determines the acidity of the catalyst. It also effects a large difference in the species distribution and quality of the cracked bitumen ^[19]. A desirable catalyst for cracking petroleum must be able to withstand the high temperature of the reactions. In the case of zeolites the higher the Si/Al ratio the better the catalyst as more silica in the framework means a more stable structure. A higher Si/Al ratio has the added benefit of distancing the aluminum sites from each other which ensures maximum acidic strength for each site ^[20, 21].

The most common use in the petroleum industry for zeolites is as FCC catalysts. Twenty years after their introduction in 1959, all catalytic cracking units used zeolites as their catalyst. The FCC process is intended to crack heavy oil fractions into lighter ones, but not too light, as the optimal product is made up of the middle fractions. Zeolites were used due to their ability to maximise the generation of valuable middle fractions while limiting the generation of unwanted light gases and coke due to overcracking ^[22]. Zeolite Y, the first industrial zeolite, had the sodium cations exchanged with rare earth metals to stabilize the zeolite structure

and protect the acid sites ^[23, 24]. In 1986, laws were passed to remove lead from gasoline which required higher octane levels to compensate. This was accomplished by lowering the aluminum content of the zeolite ^[24]. With the aluminum content lowered, the zeolite framework became more stable and the new catalyst was called Ultra Stable Y (USY). This zeolite can be exchanged with rare earth elements as well, creating Rare Earth Ultra Stable Y (REUSY). The different zeolites are used according to which final products the producer desires.

1.4 Catalytic Cracking Using Natural Zeolites

The novel idea of using natural zeolites for catalytic cracking was not explored until Dr. Kuznicki's group started to experiment with two types of zeolites, clinoptilolite and chabazite. One of the benefits of using natural zeolites is their abundance, which makes them very cheap and economical to use. Experiments conducted by Dr. Kuznicki's group have focused both on natural and upgraded-natural zeolites ^[25, 26].

1.4.1 Proof of Concept Studies Using Microreactors

Due to the aforementioned benefits of natural zeolites and the interest in improving current methods used to extract oil from the oilsands, Dr. Kuznicki's group focused on the use of zeolites for cracking of Athabasca oilsands. Oilsands

and the zeolite were reacted in small microreactors at temperatures lower than normal thermal cracking and then extracted using light hydrocarbons ^[25]. The benefits of such a process are myriad, including the efficiency of the inexpensive catalyst, possible upgrading effects and the environmental aspect. The possibility of extracting the oil using pentane or other light hydrocarbons instead of water would remove the largest environmental concern for the oilsands, the tailings ponds. In addition, zeolites were also found to exhibit upgrading benefits; they lower the viscosity and remove heavy metals during the reactions ^[26].

1.4.2 Stirred Reactions

To improve the mass balance, feed-catalyst contact, and to generate enough product for further analysis, a scaled up and redesigned system was needed. A larger, 1 L, stirred autoclave with a special helical-scraper impeller to improve the oilsands-catalyst contact was designed. In a previous study, conducted with clinoptilolite and using this new system, it was found that a small addition of water, 3 %, would aid in the catalytic cracking of the oilsands. In addition, mixing during the reaction would increase the catalyst contact time, improving the reaction. It was also discovered that the zeolite catalyst did not need to be hydrogen exchanged to crack the oilsands. In fact, there was no significant difference between the hydrogen exchanged zeolite and the raw natural zeolite when water was included. Preliminary viscosity tests indicate that in the stirred reactor, zeolitic cracking drastically lowered the viscosity at reduced temperatures.

These results were promising and generated interest in a possible method for upgrading and cracking the oilsands at the same time. Extent of cracking tests, product quality tests and a rudimentary energy balance were conducted to discover the feasibility of the process. The upgrading properties of zeolites are so appealing that a study to investigate the ability of zeolite to improve the quality of pre-extracted bitumen was also performed.

Chapter 2. Experimental

The experimental work was divided into two main areas: the stirred oilsands reactions and the bitumen reactions. The stirred oilsands reactions focused on determining the cracking effect of a natural zeolite catalyst when combined with the oilsands and heated up to moderate temperatures, leading to a proposed industrial extraction and upgrading process. The bitumen reactions were conducted to investigate the upgrading effects of natural zeolites when combined with industrially extracted bitumen and heated to relatively low temperatures.

2.1 Materials

2.1.1 Feed Components

Pit mined oilsands were procured from the Mildred Lake facility by Syncrude. It was classified as a medium-high grade oilsands with few rock impurities.

A number of different types of bitumen are used in the bitumen tests. For the first test, to determine the optimal catalyst loading percentage, industrially extracted bitumen from Syncrude was employed. For the rest of the tests, bitumen extracted from the oilsands received from Mildred Lake, the same as the oilsands used in the stirred oilsands reactions, was used. The bitumen was extracted from the oilsands using the same extraction process used to extract the bitumen after the cracking reactions, described in section 2.3.

2.1.2 Catalyst and Control Material

The catalyst used in these experiments was calcium rich chabazite, a naturally occurring zeolite procured from Bowie, Arizona. In the catalytic effect set in the bitumen reactions, silica dried from a Ludox HS Colloidal 40 wt% silica water solution was used as a control material. The materials were all less than 0.075 mm and in their raw form.

2.1.3 Catalyst Characterization

Four different characterization tests were done on calcium chabazite and, as a comparison, zeolite Y.

X-Ray Diffraction (XRD) analysis was performed using a Rigaku Geigerflex 2173 diffractometer, using a Co radiation source, with a vertical goniometer equipped with a graphite monochromator. The data was processed using XRD pattern processing software Materials Data Jade version 7.5, and matched with JCPDS data base Powder Diffraction Files (PDFs).

Scanning Electron Microscopy (SEM) pictures were taken using an Auger microprobe JAMP-9500F spectrometer from JEOL equipped with a Schottky field emission source. The pictures were taken in an ultra high vacuum.

The catalyst surfaces areas were measured using the Brunauer, Emmett and Teller (BET) method used on nitrogen adsorption isotherm data obtained at liquid nitrogen temperature with an Omnisorp 360 Analyzer.

Energy Dispersive X-Ray (EDX) data was collected using a PGT PRISM IG (Intrinsic Germanium) detector attached to a Hitachi S-2700 Scanning Electron Microscope equipped with a PGT (Princeton Gamma-Tech) IMIX digital imaging system.

2.1.4 Dean Stark Analysis

Further characterization of the oilsands feed was done via the Dean Stark analysis to determine its water, bitumen and solids content. The analysis was performed according to the ASTM D95 standard ^[27]. The method is used to determine the amount of water innately found in the oilsands, also known as the Koenig water. The experimental setup can be seen in Figure 2-1.

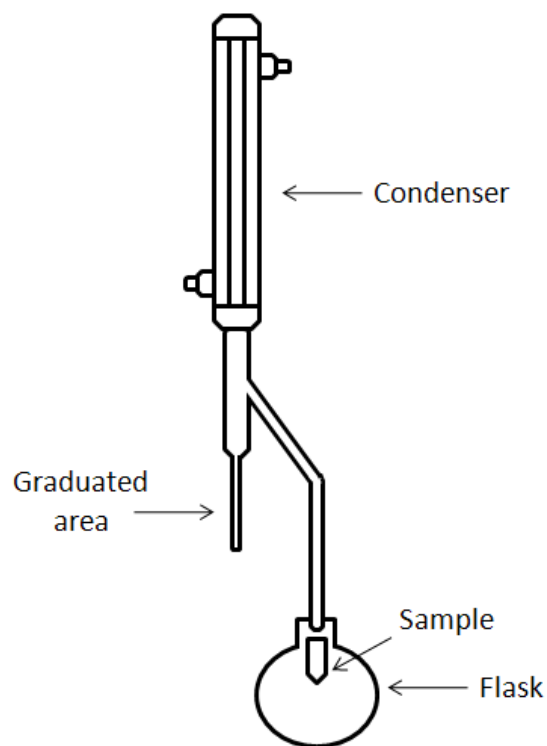


Figure 2-1 – Dean Stark analysis experimental set up.

Before performing the procedure, all pieces of the apparatus were carefully cleaned. The amount of water present in the oilsands is small and so great care was taken before the experiment to clean the graduated area so that the water falls to the bottom and does not adhere to the sides of the piece. Toluene was then poured into the bottom flask and a small amount of sample was loaded into a filter paper and thimble combination. The thimble was hung in a wire cage in the bottom flask below the connection between the receiver piece and the flask but not touching the solvent. When the heat was turned on, the toluene boiled and its

vapours rose and cooled in the condenser. There they fell into the receiver's graduated section which, once full, dripped down back to the bottom flask landing on the sample. The toluene would then strip the sand of the bitumen and water, which would fall into the bottom flask. Since the boiling point of toluene is 110 °C, the stripped water would also boil and follow the path of the toluene. Keeping in mind that water has a higher density than toluene, after it had condensed; the water would fall and become trapped in the graduated portion of the receiver. After 6 hours, the procedure is assumed complete and the amount of water can be read from the graduated portion of the receiver.

2.2 Reactions

2.2.1 Stirred Oilsands Reactions

A 1 L stainless steel Parr reactor, equipped with a custom designed helical-scraper type stirring device, was used for the stirred oilsands reactions. A diagram of the reactor is shown below in Figure 2-2.

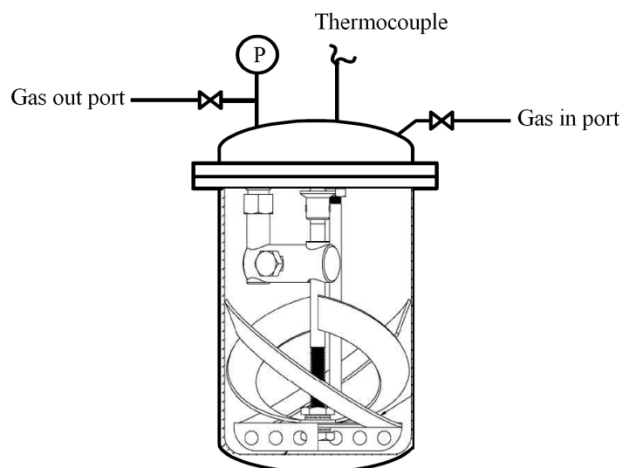


Figure 2-2 – Diagram of the stirred oilsands reactor.

The impeller within the reactor was a set of helical blades designed to ensure homogenous mixing and uniform heat distribution in the reactant mixture. As a note, the magnetic drive of the mixing mechanism, not shown for the sake of clarity, was attached to the top and center of the reactor. The thermocouple extended into the middle of the blades, ensuring an accurate temperature reading at the center of the reactor.

Prior to commencing each reaction, a graphite seal (Parr) was placed in the cleaned sealing ring in the top part of the reactor. The oilsands were then measured in plastic measuring trays, 100 g to a tray for a total of five trays. The amount of catalyst needed for that run was calculated, divided by 5, and measured directly into the same trays as the oilsands. Each tray was then individually put into a mortar and mixed with the pestle until just before the mixture began to stick

to the mortar. Once all the individual trays were mixed, the oilsands and catalyst were put into the reactor. This was done by lifting the top piece of the reactor and the stirring mechanism out of the bottom piece of the reactor. The trays of oilsands were then shaped and placed between the mixing blades. This was done because the large geometry of the stirring blades made it impossible to put the reactants in and then the top piece and mixing blades. When all the reactants were put between the blades, the mixing mechanism and top piece were lowered back into the reactor. The reactor was then sealed and pressurized to 1850 kpa with helium gas (4.5 pp, Praxair). The reactor was then checked for leaks by submerging it in water. Any bubbles escaping the reactor indicated that there was a leak. Once the reactor was confirmed to be sealed, it was taken out of the water. The pressure was then let out and 15 g of deionized water was then injected, via a syringe, into the reactor through the 'gas in' port. The helium gas was reconnected to the 'gas in' port and then the reactor was pressurized to 550 kpa to ensure the water was sprayed into the main part of the reactor. The gas was released and the reactor pressurized again. This sequence was repeated seven times to ensure that no air remained in the reactor, as this would have allowed combustion and other unwanted reactions. Once the seven cycles were complete, the pressure was reduced to just above ambient pressure. The reactor was then placed into an insulated heating furnace equipped with a Parr 4843 PID controller, presented in Figure 2-3. The controller commands both a PID for the heater and also manages the mixing speed, which was set to 90 rpm for all the runs.

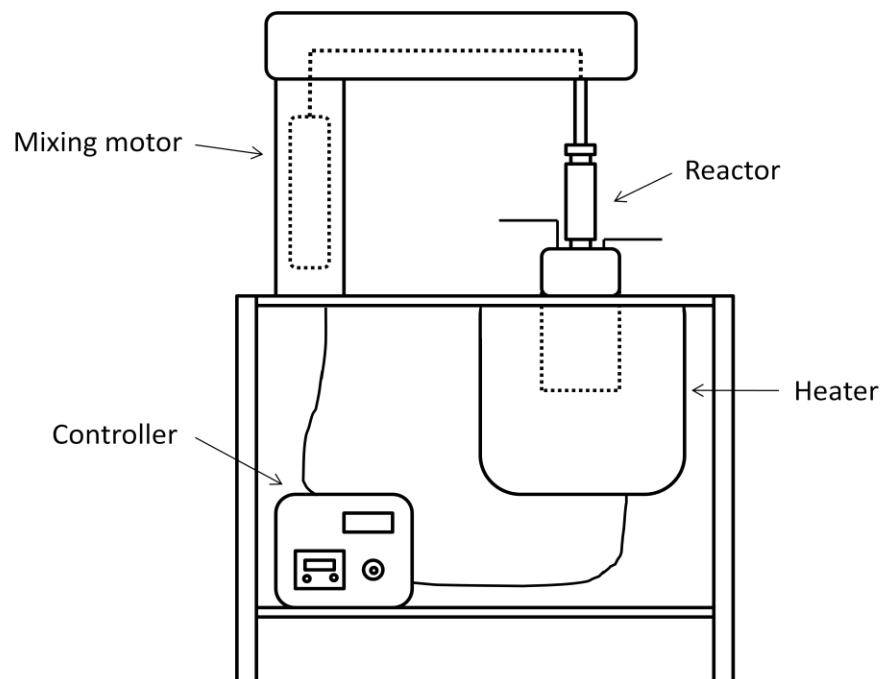


Figure 2-3 – Diagram of the reactor in the heating mantle, PID controller and the mixing apparatus.

The temperature of the reaction was controlled by a thermocouple inside the heating mantle, next to the outside wall of the reactor. The temperature recorded as the reaction temperature was measured by the thermocouple inside the reactor. Initial trial and error runs were performed to find the required setpoint temperature, controlled by the heating mantle, to ensure the desired inside temperature of the reactor was achieved. This process was closely monitored due to high pressure and difficulty controlling the temperature profile, both stemming from the superheating of water and the outside wall temperature always being substantially higher than the desired reaction temperature. For example, for a

300 °C reaction temperature, the PID controller setpoint of the heating mantle was set to 350 °C; while for a 350 °C run, the setpoint temperature was 415 °C to 450 °C, depending on the run. It should be noted that this caused the walls of the reactor to be at a higher temperature than the internal reaction temperature. The high mixing speed was also used to ensure that sample was not left to overheat touching the wall. Once the internal reaction temperature achieved its setpoint, the reaction was allowed to continue for 1 hour.

A series of experiments for the stirred oilsands reactions was prepared with reaction temperature and catalyst loading as the two variables. The points of the matrix were a combination of temperature (300 and 350 °C); and catalyst loading, (0, 1, 3 and 5 %). The catalyst loading was defined as a weight percentage of the oilsands, eg. If 500 g of oilsands were used, a 5 % run would contain 25 g catalyst. A run of 0 % catalyst was a thermal reaction without catalyst, used as a control run. All runs in the stirred oilsands reactions were done with an addition of 3 % water based on oilsands weight. The design of experiments was intended to determine the optimal reaction conditions in terms of yield and product quality.

After the prescribed 1 hour reaction time, the reactor was quenched in tap water to stop the reaction. The water level was set below the collar to prevent it from warping the sealing area. The reactor was left to cool in the water until the internal temperature had returned to room temperature, after which the temperature and pressure of the reactor were recorded. The reactor's gas outlet

was then connected to the Gas Chromatograph (Shimadzu) to analyze the gaseous products of the cracking reaction, in the range of C1-C4, and these results were recorded as the gas products.

To prevent the loss of any products with low boiling points during handling, these light fractions were collected from the cracked product. The reactor was placed back in the heater and heated to an internal temperature of 150 °C. Heating tape was placed around all the external pipes of the reactor to prevent any light fractions from condensing where they could not be recovered. Helium was used to sweep the now gaseous light fractions into a cold trap which was maintained in an ice water bath to condense all the light fractions. The condensate-free gas was then passed through two bubblers containing NaOH dissolved in water to trap any H₂S coming out with the gas for safety reasons. This process was run for 3~5 hours until no more light fractions were seen condensing. The products, light liquid hydrocarbons and water, were then separated by density difference and individually weighed in vials. The hydrocarbons were recorded as the condensate products and stored in a freezer to prevent loss. The reactor was allowed to cool overnight.

The following day, the cracked products were removed from the reactor, weighed and stored in a 0.5 L glass container kept in a freezer.

2.2.2 Bitumen Reactions

The series of experiments performed on bitumen were done in custom made Swagelok micro reactors. For these experiments, there were 3 different sets of runs.

The first set of experiments, the loading effect set, was performed on 3 g of industrially extracted bitumen and varying amounts of the chabazite catalyst at a reaction temperature of 400 °C. The levels of catalyst used were 0 (a thermal reaction), 10, 25, 50, and 100 weight % of the bitumen added. This series of tests were used to determine the optimal catalyst loading percentage. The reaction time was 40 minutes and the reactor quenched in water to stop the reaction.

The next set of experiments, the reaction time set, was designed to explore the effect of time on cracking reactions. The reactions were conducted with 10 % water, and 10 % catalyst and a set of thermal control runs were also performed. The reaction times were 1, 4, 16 and 48 hours. A lower temperature of 300 °C was selected to prevent overcracking during the long reaction times and also to observe the upgrading effects of prolonged low temperature on bitumen.

The final series of experiments, the catalyst effect set, were conducted to test the reusability of zeolites. The experiments were performed at 300 °C with 10 % water and 10 % catalyst loading for 48 hours. The materials used were chabazite and, as a control, silica. Following each reaction and extraction the catalysts were recovered and reused in a second cycle with fresh bitumen (explained in section 2.3).

Due to the small amounts of components used, the bitumen, catalyst and water were carefully measured and combined in the micro reactor as opposed to a weighing pan. The reactor was then sealed and pressurized with 4.5 pp grade He to 1380 kpa and released. The pressurizing and venting cycle was repeated seven times to ensure no air remained in the reactor.

The sandbath, shown below in Figure 2-4 with the shaker assembly, was fluidized with an air flow at a rate of 1650 L/h, to maximize the heat transfer. The fluidized bath's heater was then turned on, controlled via a simple custom PID controller, and allowed to reach equilibrium at the designated temperature, 10 degrees more than the reaction temperature to allow for thermal incline. The reactor was secured to the metal rod connected to the shaker arm, inserted into the sandbath, and then the shaker assembly was activated.

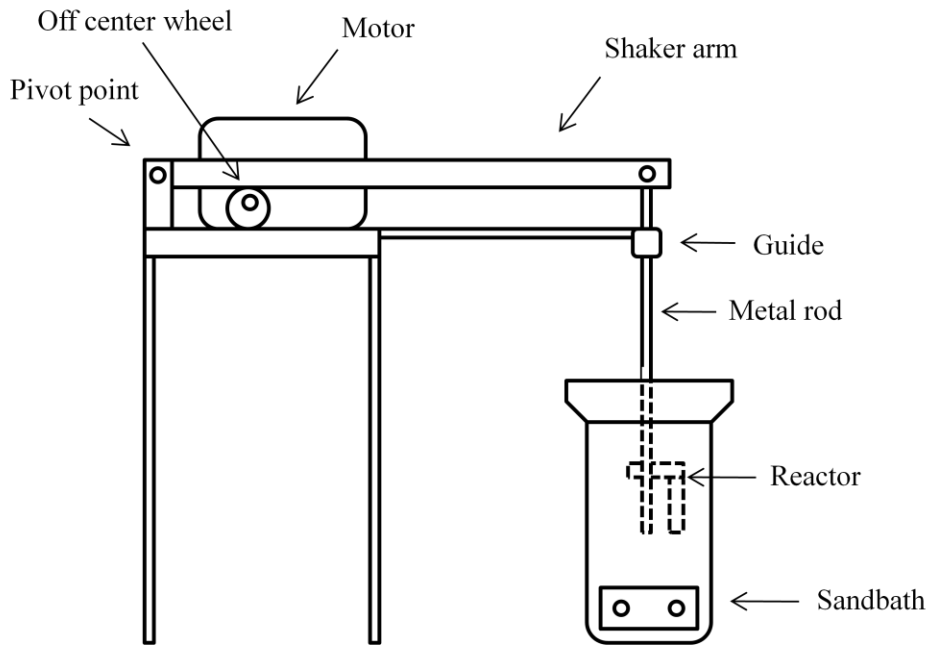


Figure 2-4 – Shaker assembly with reactor placed in sandbath.

The assembly consists of a shaker arm attached to a pivot point on a metal table, which is bolted to the ground to avoid shifting. A motor driving an off center wheel, on which the shaker arm rests, provides the up and down motion for the mixing of the catalyst and bitumen. Once the reaction time had passed, the reactor was removed from the sandbath and cooled by a stream of compressed air, except for the loading effect runs as previously mentioned, to room temperature.

2.3 Extraction

The general process of extraction was the same for the pentane and the C5 asphaltenes extraction of the solid oilsands, and the toluene extract of the liquid bitumen reactions. The specific variations of each process's extraction are described after the main process.

The cracked products are placed in a single thickness cellulose thimble containing a folded filter paper receptacle (Whatman #4) which is used to retain the sand and catalyst but let the solvent and product through. After which the thimble was put into the soxhlet extractor. In the case of the bitumen reactions, the microreactor was washed and rinsed with toluene and poured into the thimble to ensure that no product or catalyst was lost. Additional solvent was added as required to the bottom flask, to the required total of 500 mL solvent which ensured complete extraction of the bitumen. For oilsands extractions, the full amount of solvent was added to the bottom flask directly as there was no need for washing. The

solvent, pentane or toluene, was then heated to its respective boiling point using FisherSci heating mantles. The gaseous solvent then passes up the tube and condenses on the condenser mounted on top of the soxhlet apparatus and drips down onto the cracked sample. For these heaters, the required settings were found to be 4 for pentane and 7.5 for toluene. This ensured that the solvents were at their boiling temperatures and the condensing solvent was dripping at a rate of 2-3 drops a second. Once the heater was started, the extraction was run for 6-8 hours to ensure all the products were extracted.

Once separated from the catalyst and sand, the products were in solution and needed to be separated from the solvent. The solvent was removed from the products using a Büchi R-200 rotovapor with an attached Büchi B-490 heating bath. The flask was heated to 40 °C for pentane and 60 °C for a toluene sample. In addition to the heat, a vacuum was applied to the toluene extracted sample to aid the evaporation. The solvent vapour was condensed by cooling water running through the upper receptacle. The process was complete when no more solvent was seen condensing. To transfer the products from the glass flask to a weighing pan, a small amount of solvent was required. Once the products were moved, the pan was dried overnight in an oven at either 40 °C or 110°C, for pentane and toluene respectively, to remove the added solvent. The following day the samples were then weighed to measure the amount of pentane extracted product or C5 asphaltenes product for the stirred oilsands reactions, or toluene extracted product for the bitumen reactions.

For the catalytic effect experiments, the materials were recovered for reuse in a second set of reactions. At the end of the usual extraction process, the thimbles were left with only the catalyst remaining as all the bitumen was extracted by the toluene. To recover the catalyst, the thimbles were dried overnight at 110 °C to evaporate any residual toluene. The following day, the filter paper was carefully extracted from the thimble and then the catalyst was lightly shaken out of the filter paper onto a weighing paper. Due to the very small size of the catalyst grains and the small amount of catalyst present, approximately 36% of the catalyst was lost during the recovery process so two runs were required to have enough catalyst for each reaction in the second level of runs.

2.4 Coke

To determine the amount of coke produced during the stirred oilsands reactions, the sand was put into crucibles able to withstand high temperatures. The crucibles were weighed and then inserted into a Thermolyne 79400 tube furnace and heated to 250 °C under helium flow to ensure all the solvent and moisture were driven off.

The crucible was then quickly weighed again and put into a Barnstead/Thermolyne 30400 muffle furnace and heated to 800 °C for 5 hours, in presence of oxygen, to combust the coke present on the sands and catalyst. The oven was set to cool to 110 °C and afterward the amount of coke burned off was measured immediately after removal from the oven.

2.5 Viscometry

The viscosity was measured by transferring the toluene extracted samples into the cup of the bob and cup type (chamber and spindle) receptacle of a rotational Brookfield DV-E viscometer, shown in Figure 2-5 below from a side view.

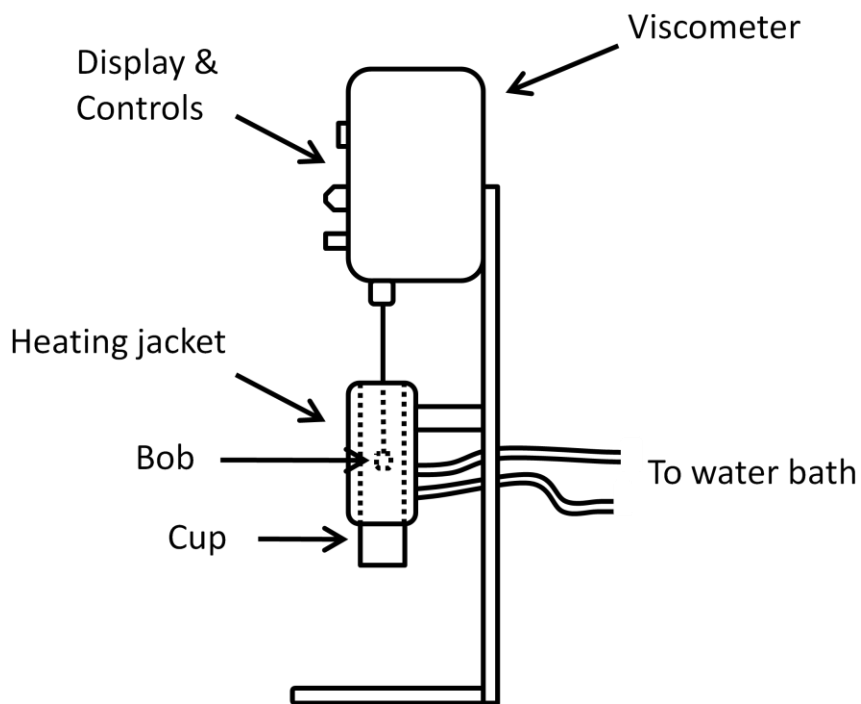


Figure 2-5 – Viscometer with the bob and cup inside the heating jacket.

After placing the bob into the sample in the cup, the receptacle was then placed into the heating jacket of the viscometer. Hot water from a water bath was used to heat the sample and the receptacle to the desired temperature through the jacket around the cup. The sample took one hour to reach thermal equilibrium after reaching the measuring temperature. The viscosity was measured at 3 different temperature points, usually 50, 55 and 60°C, for each sample. Higher

temperatures were used as required when the products were too viscous to be measured at the standard temperatures. At each temperature, 4 viscosity measurements were taken at two minute intervals from each other at the lowest rpm setting possible. This was determined by keeping the motor work percentage in between 10 and 90 %. Once the 4 measurements were taken, the rpm was then switched to the next highest setting and 2 more measurements were taken. The last set of 2 measurements was taken at the next highest rpm setting after that. At higher viscosities, the lowest rpm was sometimes the only viable measurement speed as the higher rpm were above the 90% motor work percentage, and hence were not reliable.

The measurements were taken at 3 different temperatures to collect enough data points for linear regression so that the viscosities could be compared at a common temperature. Before linear regression could be performed, the temperature and viscosity must be put through the following respective equations.

$$y = \ln (\ln(\textit{viscosity})) \quad [2.5.1]$$

$$x = \ln (\textit{temperature}) \quad [2.5.2]$$

With the new x and y variables, regression was performed to determine the a and b values for the linear equation which would allow us to extrapolate the viscosity to any range required for comparison.

$$y = ax + b \quad [2.5.3]$$

All viscosity values reported were measured at or converted to 50 °C values.

2.6 SARA Fractionation

For the SARA Fractionation analysis, the ASTM D 2007 ^[28] standard was followed with one small modification to separate the resins and asphaltenes of the polar phase. This modification was performed at the beginning by dissolving 4 g of the toluene extract of a run in 160 mL of hexane. The sample was then put in a sonic bath for 45 min. Every 10 minutes therein, the bath was stopped and the stopper retightened to prevent any escape of the solvent. After the 45 minutes had elapsed, everything barring the C6 asphaltenes, which had precipitated, was assumed to be dissolved. The asphaltenes were then separated from the sample using a Millipore set up, shown below in Figure 2-6.

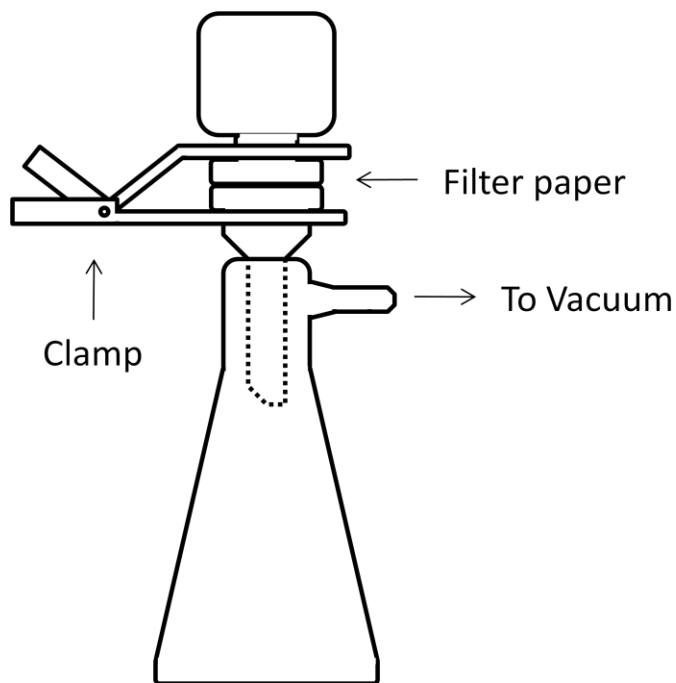


Figure 2-6 – Millipore asphaltenes extraction set-up.

The Millipore filter paper was weighed and placed in between the top and middle pieces, which were held together solely by the clamp. Once all was secure and the vacuum turned on, the sonicated sample was slowly poured into the top receptacle. Care was taken to avoid pouring on the walls of the receptacle and keeping the fluid level low in the top piece, as rinsing the asphaltenes off the upper walls and onto the filter paper is difficult. Once all the initial solution was poured out, additional hexane was added to the initial sample holder to rinse it and the walls as required ensuring, as much as possible, that all the asphaltenes were on the filter paper. The last rinse of the initial sample holder was done with heptane to ensure there was no residue left. The clamp and the top piece were then carefully removed, so as to not disturb the asphaltenes, and the filter paper slid off the bottom piece into a pre-weighed drying pan. The filter and asphaltenes could then be dried at 110 °C overnight then measured and the weight of the asphaltenes recorded. The rest of the sample, collected in the bottom flask, was also dried, but via a flow of lab air blown into the flask to remove all the solvent but not affect the product distribution. All the previous solvent must be removed as different solvents were used for the next steps and the heptane may interfere with the measurement. The ASTM procedure was followed after this point and commenced with the apparatus below in Figure 2-7.

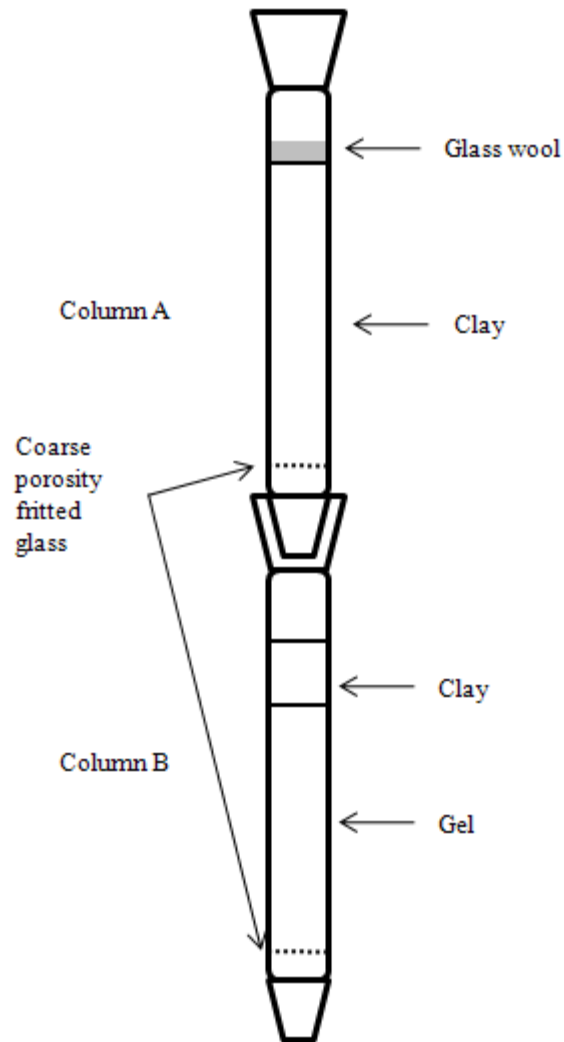


Figure 2-7 – Column set up for the SARA fractionation test.

The top column, column A, was filled with 100 g of clay, topped by a plug of glass wool to reduce the impact of the falling solvent on the clay. The bottom column, column B, was first filled with 200 g of silica and then 50 g of clay on top of that. Both columns were settled before attachment by tapping them 10 times along the sides and 25 times on top with a rubber hammer. The columns

were then attached and the bottom inserted into a graduated Erlenmeyer flask, labelled flask I.

The sample was then dissolved in 25 mL pentane while another 25 mL of pentane was added to the top column. While adding solvents to the column, care was taken to ensure that there was always a moderate amount of head above the glass wool plug to ensure that the clay bed did not dislodge itself. Therefore before the head ran out, the sample dissolved in pentane was added to the top of the column. This was followed by more pentane, ensuring that the initial sample holder and top walls of the top column were washed clean, until approximately 280 mL of pentane were collected in flask I, this was the saturates portion.

The columns were then separated; column B was allowed to continue draining, while column A was put into its own bottom flask, marked flask II. More pentane was added to the top column, maintaining a head of 2.5 cm until 150 mL were recovered, then no more pentane was added. Once the pentane had flowed through the column, flask II was put aside.

Column A was then attached to a separatory funnel and a mixture of 50:50 acetone/toluene was added in the same manner the pentane was. This mixture was added until the effluent became clear. The column was then allowed to fully drain into the separatory funnel. Once done, the separatory funnel was sealed and swirled to allow any water to collect at the bottom, which was then drained off. Anhydrous calcium chloride, 10 g, was added to the funnel, which was then

shaken for 30 s. The mixture was then filtered into flask III and the funnel and filter rinsed with pentane into the flask. Flask III then contained all the resins.

Column B was then put into an extraction apparatus where toluene was used to continually wash the clay and gel in a similar manner to the normal extraction setup. After two hours, an escape valve was opened to collect all the refluxing toluene. Once the toluene was collected, the bottom flask was allowed to cool and then combined with flask II, which became the aromatics fraction.

All the fractions were now separate, the only thing remaining was to remove the solvents, which was accomplished by placing the flasks on a hot plate set to 100 °C and left until no weight change was observed for 10 minutes.

Chapter 3. Results and Discussion

3.1 Characterization of Materials

Oilsands

The oilsands used in these experiments are from the Mildred Lake deposit in the Athabasca basin. A Dean-Stark analysis was performed and the results are shown in Table 3-1. The bitumen composition is similar to values reported in the literature ^[29].

Table 3-1 – Results of the Dean Stark analysis in weight %

Component	Wt %
Solids	86.92
Bitumen	12.08
Water	1

Calcium Chabazite

The natural zeolite catalyst used in the stirred oilsands reactions is the calcium chabazite procured from the Bowie deposit in Arizona. This natural zeolite has many interesting properties that encouraged us to look at it as a cracking catalyst, including the fact that it is cheap and plentiful.

A series of characterization tests: SEM, BET and XRD, were done on calcium chabazite and zeolite Y. Figure 3-1 below shows SEM images of chabazite and zeolite Y. The platy morphology of chabazite is readily apparent with its large, easily accessible external surface area. This is an important quality for a bitumen cracking catalyst as the large molecules, such as asphaltenes, cannot fit into the small pores of zeolite and so need to be cracked first on the external acid sites.

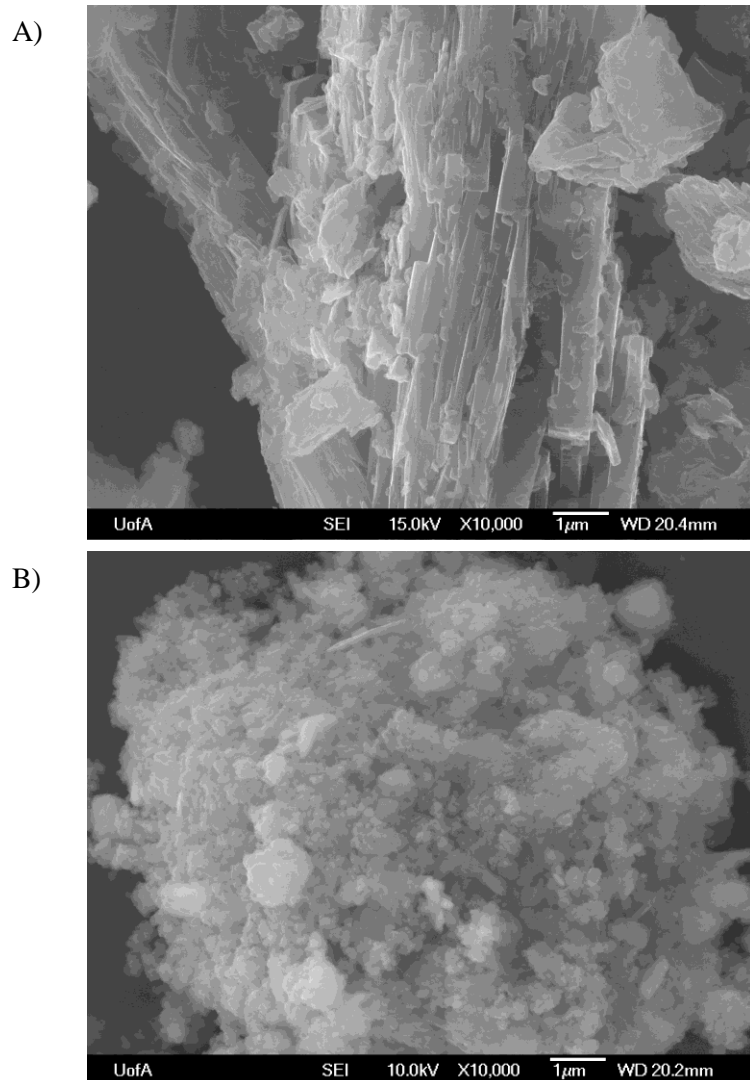


Figure 3-1 – SEM images of A) Chabazite and B) Zeolite Y.

BET analysis was used to evaluate the surface areas of the two catalysts, shown in Table 3-2.

Table 3-2 – BET and EDX analysis of calcium chabazite and zeolite Y ^[30]

Sample	BET Surface Area (m²·g⁻¹)	External Surface Area (m²·g⁻¹)	Si/Al Ratio by EDX
Ca- Chabazite	437	59 (14%)	3.6
Zeolite Y	268	78 (29%)	2.4

Calcium chabazite has a much higher Si/Al ratio than zeolite Y, an indication that the chabazite has a higher thermal tolerance and is more acidic than zeolite Y.

The external surface area of calcium chabazite is on the same order of magnitude as the zeolite Y. Taking Figure 3-1 into account, it can be seen that the external surface area of chabazite is more easily accessible than the external surface area of zeolite Y. This suggests that chabazite can perform as well, if not better, than zeolite Y.

The XRD patterns for both the chabazite and the zeolite Y are shown below in Figure 3-2.

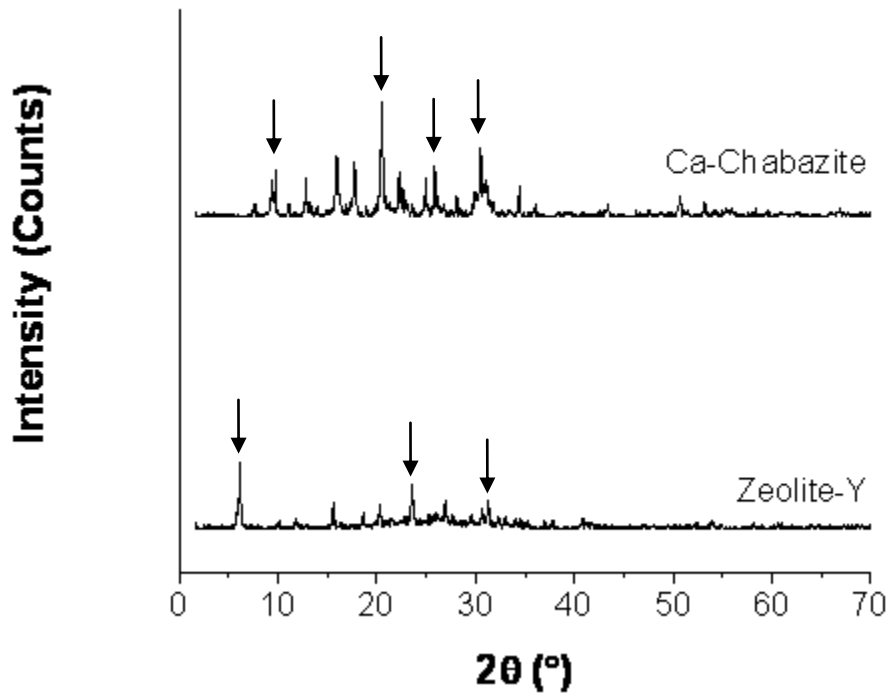


Figure 3-2 – XRD patterns of calcium chabazite and zeolite Y ^[30].

The calcium chabazite XRD pattern indicates that it is composed mostly of chabazite (indicated with the arrows), with a small presence of clinoptilolite (indicated by few peaks). The zeolite Y peaks are composed mostly of faujasite as indicated by the arrows. The very sharp, tall peaks of the natural chabazite attest to its crystallinity compared to the very low, noisy peaks of the more amorphous zeolite Y.

3.2 Stirred Oilsands Reactions

3.2.1 Product Yields

This section focuses on the recovery of different products formed during the stirred reactions: maltenes (the pentane recoverable fraction), gas, C5 asphaltenes and coke. The goal is to break the large asphaltenes molecules into smaller and more useful products but not to smaller than the maltene fraction as that would produce either coke or gas products which are not valuable to the oil industry. The yield of each product is shown as a percentage of the sum of the 4 different products in a run.

Maltene Recovery

The first set of data that was analyzed belongs to the maltenes fraction, consisting of the condensate and the liquid product recovered with pentane (Figure 3-3).

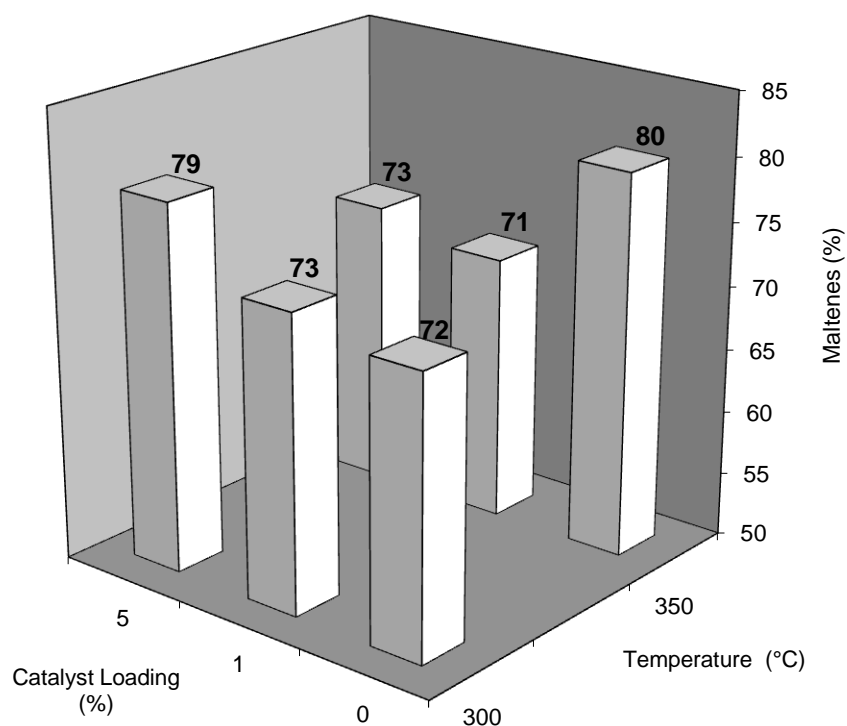


Figure 3-3 – Amounts of maltenes recovered from the stirred oilsands reactions.

Based on the percentage of the recovered maltenes it is apparent that with the addition of more catalyst the extent of cracking increases. At 300 °C as the catalyst loading is increased from 1% to 5 % catalyst, there is a 6 % increase in the maltene recovery. A higher maltene recovery is indicative of a reaction with more cracking.

The runs conducted at 350 °C in the absence of catalyst show an increase in the maltenes recovery compared to the equivalent runs at 300 °C. However, an

addition of only 1 % catalyst has the opposite effect on the return. This could be due to an increase in the amount of cracking done by the catalyst which converts the maltenes into less desirable products such as gas and coke. The idea that the catalyst could be over cracking at higher temperatures will be confirmed in the following yield sections.

There is an observable trend when comparing the catalyst loadings across the temperature difference. The 350 °C catalyzed runs are lower than their 300 °C counterparts, while higher catalyst loading yields more maltenes than lower catalyst loading in the same temperature regime. These two effects cause 5 % 350 °C to have the same return as the 1 % 300 °C run. The temperature trend is opposite in the thermal runs where increasing the reaction temperature increased the return.

As previously mentioned, the maltenes are the most valuable product from catalytic cracking. Based on these data the optimal conditions for a high product yield are low temperature but high catalyst loading.

Gas Production

The amount of gas produced during the reaction is shown in Figure 3-4.

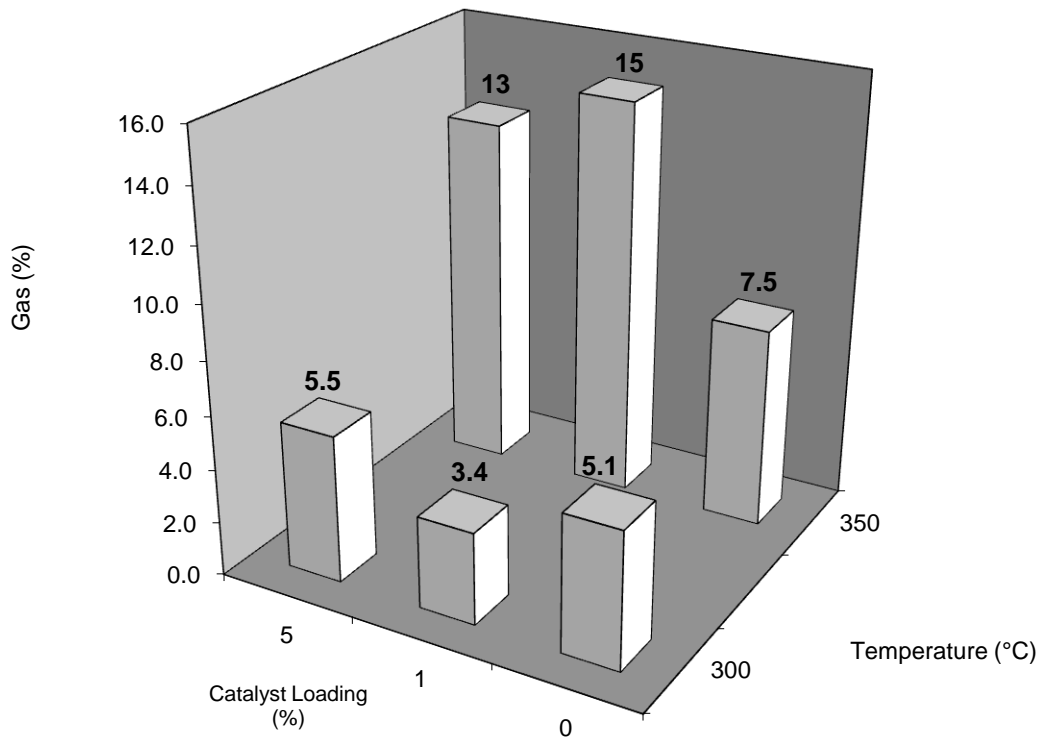


Figure 3-4 – Amount of gas collected from the stirred oilsands reactions.

At 300 °C there is little variation between the catalyzed samples and the thermal run. Which, when compared with Figure 3-3, is promising as there is no variation in the amount of gas produced but there was an increase in the amount of maltenes produced. This is beneficial as the gas fraction is not a desired product, as it is hard to capture, store and use. So far the cracking results indicate that we have been able to produce more desirable fractions without the unwanted by-products.

The large amount of gas made on the catalyzed runs at 350 °C compared to the thermal runs and the low temperature catalyzed runs is sub-optimal. This seems to suggest that there was indeed overcracking done by the catalyst at high temperatures. The maltenes fractions may have been cracked into the lighter gas fractions which are not a wanted industrial product.

C₅ Asphaltenes

Figure 3-5 shows the C₅ asphaltenes contents which are the unconverted heavy fractions from the reactions. The asphaltenes can be turned into useful products, but additional processing is required which is undesirable from an industrial perspective.

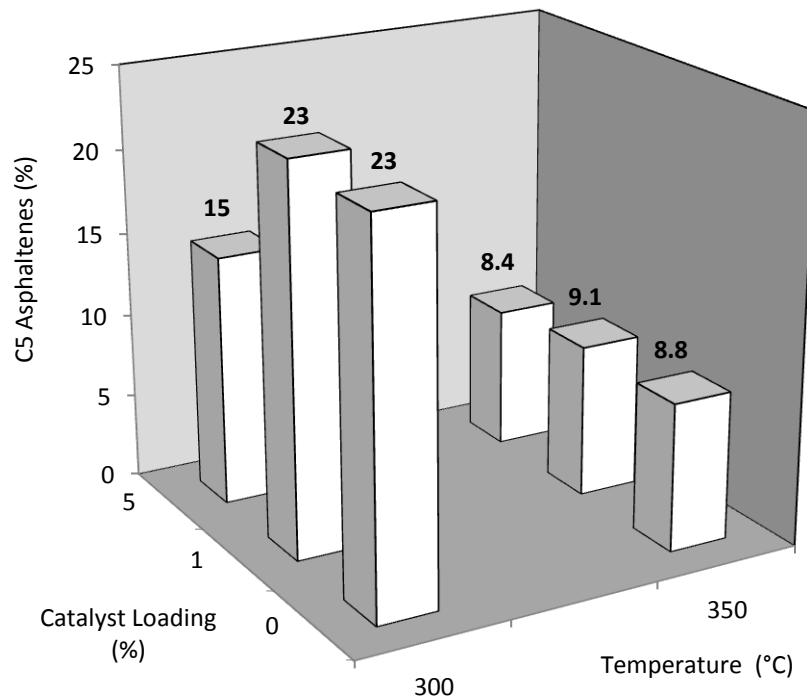


Figure 3-5 – Amount of C₅ asphaltenes left after the stirred oilsands reactions.

At 300 °C, the addition of 1 % catalyst has no effect on the C5 asphaltenes yield, which is consistent with the previous two figures where there was not much difference between these two points. The 5 % catalyst loading run on the other hand has a large drop in the amount of asphaltenes present in the product. This shows that there is an optimal loading of catalyst to obtain the maximum yield. An additional point reinforced here is that increasing the amount of catalyst increases the amount of cracking.

The asphaltenes contents at 350 °C are all fairly close; there is no evidence of the amount being cracked increasing with catalyst loading. This seems to suggest, in light of the point that increasing the amount of catalyst increases cracking, that the natural zeolite catalyst cannot crack the remaining molecules at these catalyst loadings.

Coke

Shown below in Figure 3-6, coke is another industrially unwanted by-product.

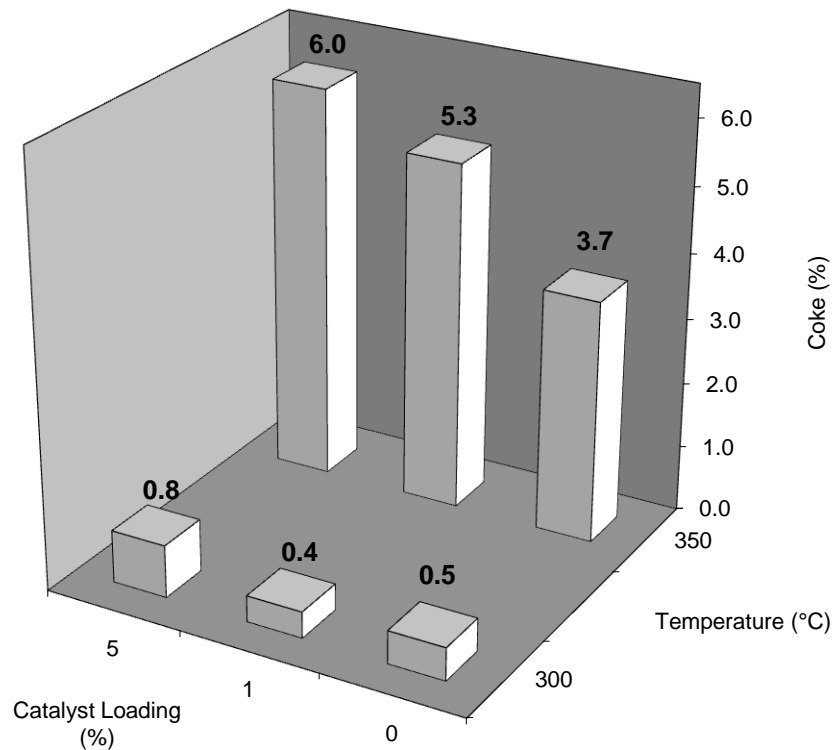


Figure 3-6 – Amount of coke generated by the stirred oilsands reactions.

There is very little variation among the low temperature runs. The thermal and 1 % loading are virtually the same; though this is to be expected as there were only minute variations in the other product yields. There is an increase at 5 % loading, but it is not significant considering possible errors associated with the experimental measurements. This is very promising as when coupled with the maltenes yield in Figure 3-3 it shows that there is substantial catalytic cracking but no overcracking.

Moving from the low temperature to the high temperature runs, it can be seen that in all the runs, the amount of coke increases significantly. This is to be expected as the reaction severity increases, the added energy can result in overcracking of the products. Similar to Figure 3-4 showing the amounts of gas, there is a jump from the thermal run at 350 °C and the 1% catalyst loading and again with the addition of 5 % catalyst. This seems to reinforce the idea that adding catalyst increases the amount of cracking where there is a steady increase with catalyst loading.

Overall Reaction Product Distribution

To aid in the understanding of all the products and how they affect each other, Figure 3-7 shows a breakdown of all the products from the cracking reactions. It is important to note that the pentane recoverable fraction has been split into its two parts, first the lighter hydrocarbons collected in the condensate phase and also the pentane extraction products, which were collected from the soxhlet apparatus. The figure sums up the previous points made above very clearly by showing the progression of cracking across the samples.

This figure also makes new points visible, such as that coke generation is not necessarily a negative indicator of the reaction products. In both temperature regimes the 5 % catalyst loadings have a higher level of coke than the 1 % catalyst loadings, but the 5 % catalyst loadings have a higher maltene yield than the 1 % loadings.

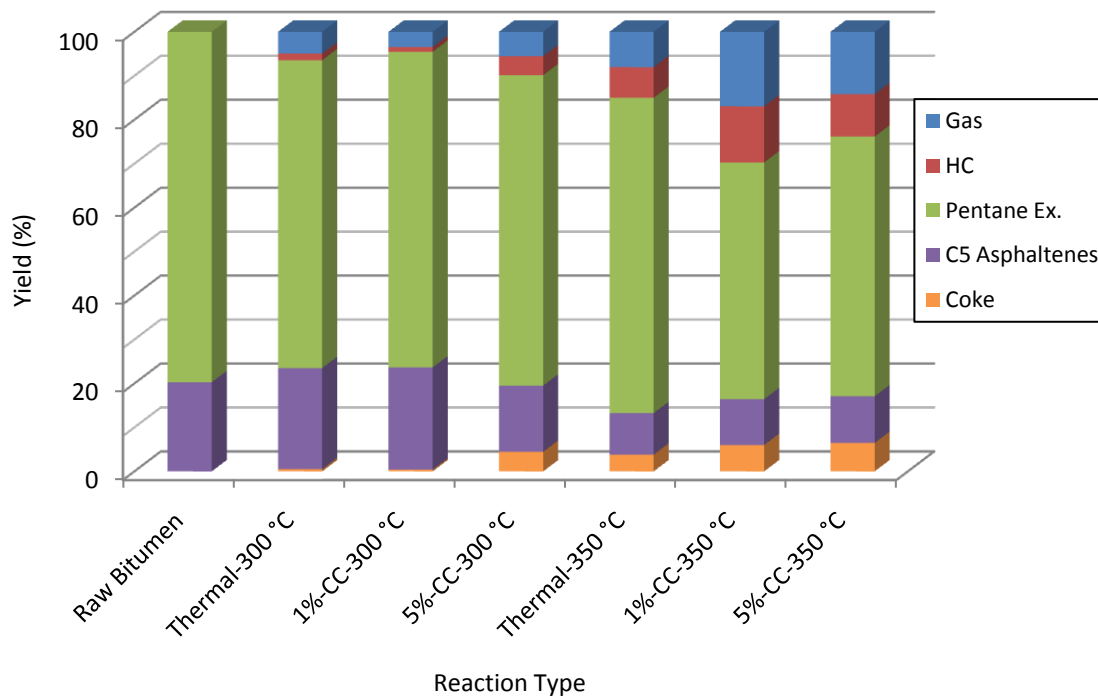


Figure 3-7 – Overall reaction product breakdown of the stirred oilsands reactions.

Error

For the yield section of the stirred oilsands reactions, a set of 2 repeat runs were conducted at 5 % loading and 300 °C shown below in Table 3-3. The error stands for one standard deviation as determined by multiple repeat runs conducted on a single sample.

Table 3-3 – Error percentages of all product yields for stirred oilsands reactions

Product	Error (%)
Gas	1.5
Condensate	0.9
P-Extract	2.9
C5 Asphaltenes	5.5
Coke	1.6

The error values are all low except for the C5 asphaltenes, which makes sense due to the very small amount collected, from 0.5 to 1 gram of sample.

3.2.2 Product Quality

The next section demonstrates the product quality from natural zeolite based catalytic reactions. The measures appear to indicate that higher temperature and catalyst loading are required to achieve the best product quality.

SARA Fractionation

The data in Figure 3-8 below summarizes our findings on distribution of different fractions in liquid bitumen products by SARA fractionation.

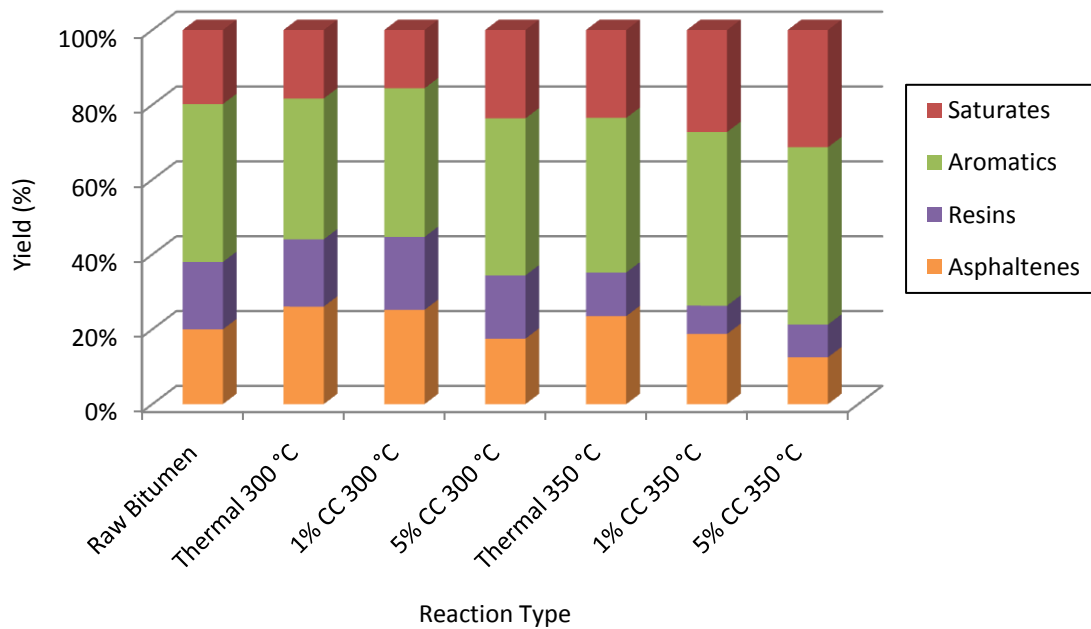


Figure 3-8 – SARA fractionation products of the stirred oilsands reactions ^[31].

The results follow the trends pointed out in the previous figures, increasing the temperature and the catalyst loading increases the amount of cracking. This is shown nicely in both the 300 °C, with 5% percent loading, and much more evidently in the 350 °C regime. In the 300 °C points, the addition of 1% catalyst has little effect on the resins or asphaltenes, but slightly increases the amount of aromatics at the cost of the saturates.

Surprisingly, there appears to be an increase in the amount of undesirable asphaltenes in some of the runs compared to raw bitumen. This can be explained by two different theories, or a combination of both. First, due to the fact that the

raw bitumen was not reacted, it did not lose any of its lighter fractions to gas or condensate, while the reacted runs did have some of their lighter products removed. Removing the lighter products has a concentrating effect on the heavier fractions due to the normalization of the SARA fractions which would result in a larger asphaltenes yield. The second theory is that this is due to polymerization reactions that occur with thermal cracking. Polymerization is the opposite of cracking and increases the amount of heavy fractions at the cost of medium or light ones.

Comparing the 5 % catalyst loaded 300 °C reaction with the higher temperature ones, it can be seen that the 5% catalyst loading at lower temperature cracks a little more asphaltenes than the 1% catalyst loaded 350 °C reaction, though the 1% catalyst loaded lowers the resin content dramatically compared to the other. The 5% catalyst loaded 350 °C reaction greatly out performs the 5% catalyst loaded 300 °C reaction in all cracking aspects, with the higher temperature reaction having the lowest concentration of asphaltenes across the figure. Looking at just the 350 °C runs, the resin concentration is the same for both catalyst loadings but the 5% has a higher amount of both aromatics and saturates.

We also begin to see a trade-off situation arising; while low temperature loadings have a better yield than the high temperature, the products from the high temperature catalyst loading are of better quality. The 1 % catalyst loaded 350 °C reaction has a higher quality, demonstrated by more saturates and less resins and asphaltenes, than the 5 % catalyst loaded 300 °C reaction. The 5 % catalyst loaded 300 °C reaction does however crack the asphaltenes into resins more than

the thermal run at 350 °C, indicating that the strength and benefit of the catalytic reactions.

Viscosity

The viscosity values of the product liquids align very well with the previous results, such as the SARA fractionation. Figure 3-9 shows the viscosities for the runs done at 0, 1 and 5% catalyst loading. All viscosity values are at a basis of 50 °C. The same trend of higher temperature – high catalyst loading yielding a higher product quality is repeated with the viscosity.

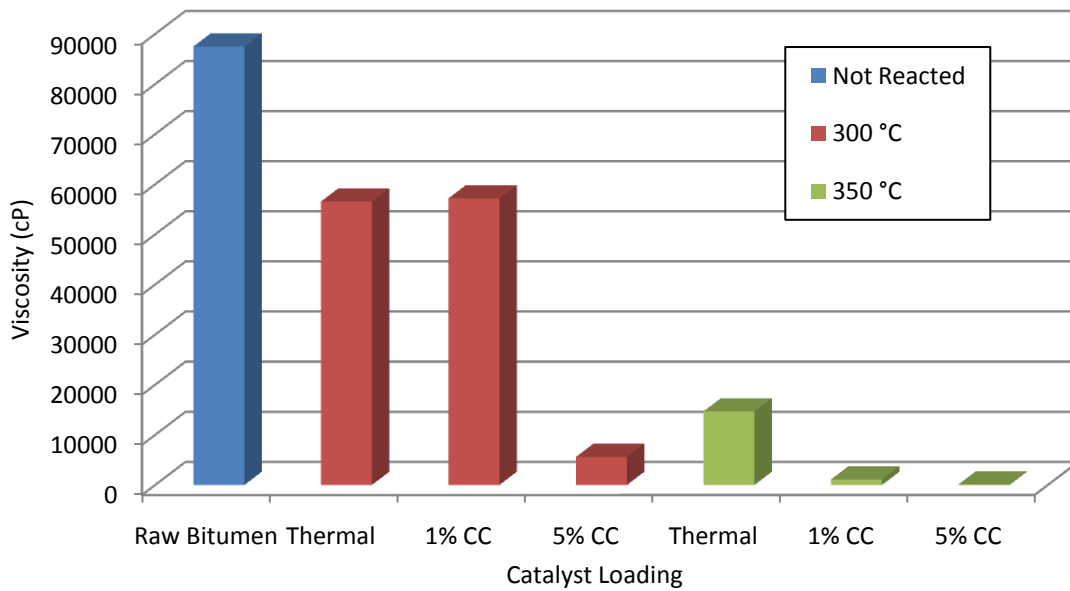


Figure 3-9 – Viscosities of the stirred oilsands reactions.

The highest point by far is the raw unreacted bitumen and once again, from there, there is a simple progression downwards with increasing temperature and catalyst loading. An important point is that the 5% catalyst loading at 300 °C has a lower viscosity than the thermal loading at 350 °C. This reveals the effectiveness of the catalyst at reducing the viscosity of the bitumen. The trends in this figure are the same as the previous one with SARA fractionation in terms of cracking.

The results in this section reinforce the product yield section in some areas, such as that the more catalyst added, the more cracking will occur. But it also introduces a significant trade off, in that while the lower temperature high catalyst loadings do improve the quality over the thermal runs, higher temperature is required to achieve better product quality.

Error

To determine the SARA fractionation test error, the same sample was run 3 times to evaluate its error. The results are shown in Table 3-4.

Table 3-4 – Error percentages of the SARA products

Product	Error (%)
Saturates	5.6
Aromatics	3.5
Resins	1.5
Asphaltenes	3.3

The viscosity error, for both here and future tests, was determined from multiple tests of the same sample and found to be 3 %.

3.3 Energy Balance

Having done the experimental tests for the stirred oilsands reactions, it was necessary to see if the process would be a viable alternative to the current extraction and upgrading process used in industry, the Clarks Hot Water Process (CHWP). With a basis of 120 g bitumen product, an approximation of the amount in 1 kg oilsands (OS), a basic comparative energy balance was performed between the conventional industrial process and our proposed industrial process based on natural zeolites. Information for the current industrial process, with the CHWP, primary froth treatment and primary upgrading being the 3 steps, was taken from Masliyah, 2011^[29]. For our proposed industrial process using natural zeolites, we imitated the laboratory process by a primary cracking unit followed by a light hydrocarbon (pentane) extraction unit similar to the one current used in

industry. A schematic of the proposed process is shown in Figure 3-10. The mass balance percentages are of total in and total out of the reaction step. The results of both processes are summarized below in Table 3-5.

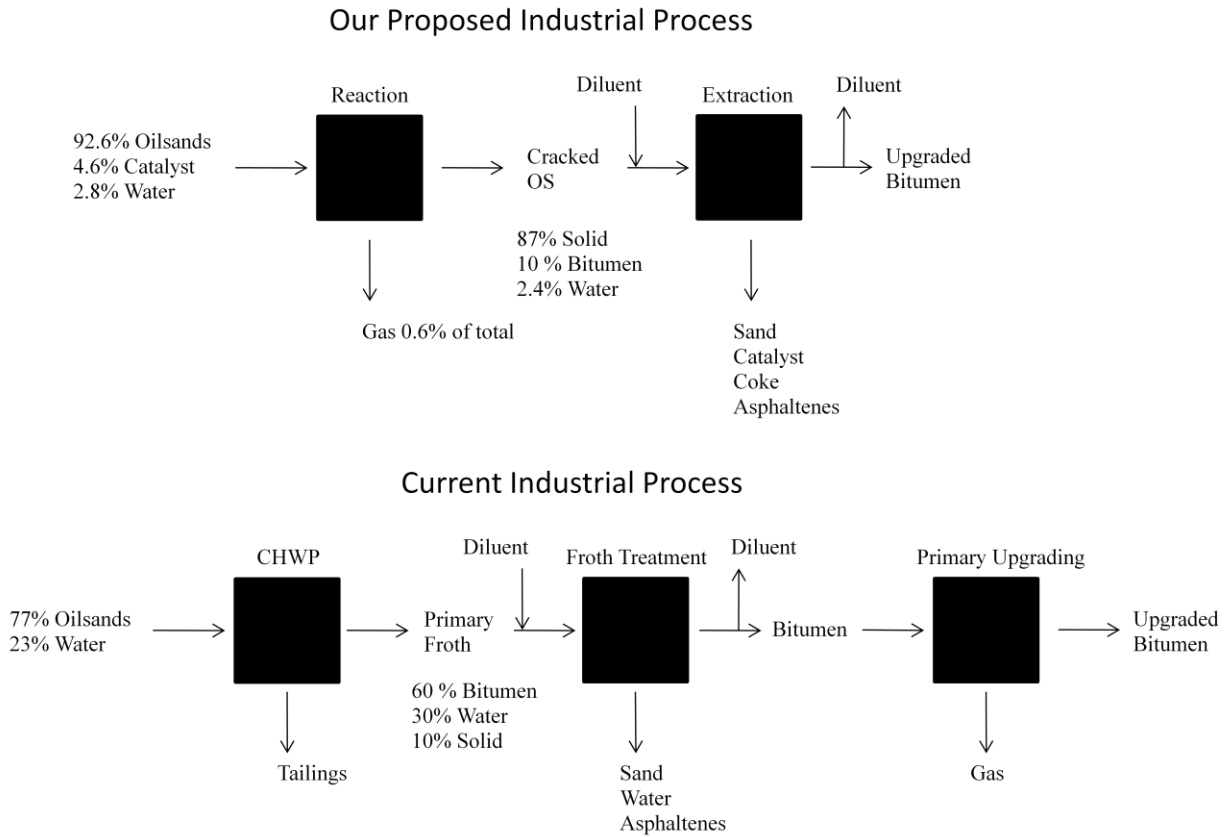


Figure 3-10 – The proposed zeolite process and the current industrial process for oilsands bitumen cracking and upgrading.

Table 3-5 – A basic energy balance around the current industrial cracking and extracting process and the proposed natural zeolite process

Weight (g)	INDUSTRIAL	PROPOSED
OS	1282	1156
Water	385	35
Catalyst	0	58
Energy (kJ)		
Heating		
OS	40	301
Water	64	104
Catalyst		15
Total	104	420
Additional steps		
Froth	140	
Upgrading	183	
P-Ex		1216
Total Energy	427	1636

The first two steps in the current industrial bitumen process, CHWP and primary froth treatment, were previously discussed in section 1.2.1. The primary upgrading step was included in the standard industrial process but was not required for the natural zeolite based integrated extraction and upgrading process. In the current industrial process, some bitumen is lost during the paraffinic froth treatment (50 % of the asphaltenes or 10 % of the incoming bitumen) and during the primary upgrading step (12 % of the incoming bitumen due to gas loss). In

the proposed process, the maltene recovery number was used (79 %) added with half the asphaltenes (7.5 %).

The proposed process in Table 3-5 was theorized at a 5 % catalyst, 300 °C and 3 % water loading. The energy section accounted only for the heating of the materials to the reaction temperature. The froth treatment method evaluated, in the current industrial process, was the paraffinic treatment method due to its solvent being similar to our proposed process. The pentane ratio used in the proposed process was 20:1 compared to the excessive 40:1 used in the laboratory in order to ensure that all the products were captured efficiently. This ratio, used for the total energy calculation, is explained further on and is based off the 2.3:1 solvent to solid ratio used in the industrial paraffinic froth treatment method used by Shell.

Judging by the weights of the reactants going into each process, it would seem that the CHWP would be the more energy intensive process, as it uses 10 times the water of the proposed process. This is more than mitigated by the fact that the CHWP is run at 60 °C while the proposed is run at 300 °C. It is interesting to note that the amount of water in the proposed process is less than 3 % of all the reactants weight while the energy to heat that small amount of water is one quarter of the total energy required. In addition, the proposed process only used 1/10 of the water of the CHWP, but required almost double the amount energy to heat that fraction of water compared to the CHWP. In this section of the energy

balance, the CHWP requires a total of 104 KJ while the proposed process needed 420 KJ.

In the additional steps of the proposed process, the amount of pentane used has a very large impact on the amount of energy used. The laboratory ratio of 40:1 required an unrealistic amount of energy. If the cracked oilsands from the proposed zeolitic process could use the same ratio as the paraffinic process then they would have the same energy requirement since they both use pentane as the solvent. The proposed cannot be performed at the 2.3:1 ratio either as there is still a large amount of sand with the bitumen. We determined that a ratio of 20:1 could be used for the solvent to bitumen ratio in the proposed pentane extraction by comparing the amount of solids in the current industrial process with the amount of solids in our proposed industrial process. The percentage of solids entering the industrial froth treatment section is 10 %, while in the proposed process it is 87%. A simple ratio of solvent to weight % solid shows that a 20:1 diluent to solvent ratio for the proposed process should dissolve all the bitumen effectively.

$$\frac{2.3}{10} * 87 = 20 \quad [3.3.1]$$

With the solvent ratio set, the total energy for the proposed industrial process becomes 1636 KJ per 120 g bitumen while the current industrial process uses only 427 KJ.

However, there are many benefits to our proposed natural zeolite cracking process. First, it eliminates the need for a primary upgrading step, due to the aforementioned upgrading effect, which will reduce the initial capital costs for the industrial plant. It also creates a reject stream with very little water, 1/10 the water of the current process, which will greatly reduce the amount of water sent to the tailings ponds. Another benefit is that the bitumen is much less viscous immediately after the first step instead of the third, facilitating the intermediate handling and reducing the amount of wear and tear on the process equipment.

While more work needs to be done to determine a more energy efficient way of using natural zeolites as cracking catalysts, a different avenue worth exploring might be to use the catalyst for upgrading pre-extracted bitumen. An additional energy balance shown in Table 3-6 shows the standard and the proposed bitumen upgrading processes.

Table 3-6 – A basic energy balance for both the current industrial upgrading process and the proposed zeolitic upgrading process

Weight (g)	INDUSTRIAL	PROPOSED
Bitumen	136	129
Water	0	13
Catalyst	0	13
Energy (kJ)		
Bitumen	162	78
Water	0	39
Catalyst	0	3
Total	162	121

The comparison was done between the current primary upgrading process, fluidized coking, and a proposed bitumen upgrading reaction using 10 % catalyst at 300 °C and 10 % water. The basis was 120 g bitumen product again. From the data it can be seen that our proposed process uses less energy than the current industrial process, even with the inclusion of water. The temperature difference of 200 °C is enough to ensure the energy efficiency of the proposed method compared to the current process. This was encouraging enough that we performed further experiments to determine if this process could indeed be a viable alternative to the current industrial process.

3.4 Bitumen Reactions

After determining that natural zeolites based bitumen upgrading is more energy efficient compared to the current industrial process, we focused on exploring the bitumen upgrading that is the subject of this section.

Optimal Catalyst Loading

In the Figure 3-11 the effect of catalyst loading was studied with runs performed at 400 °C on industrially extracted bitumen.

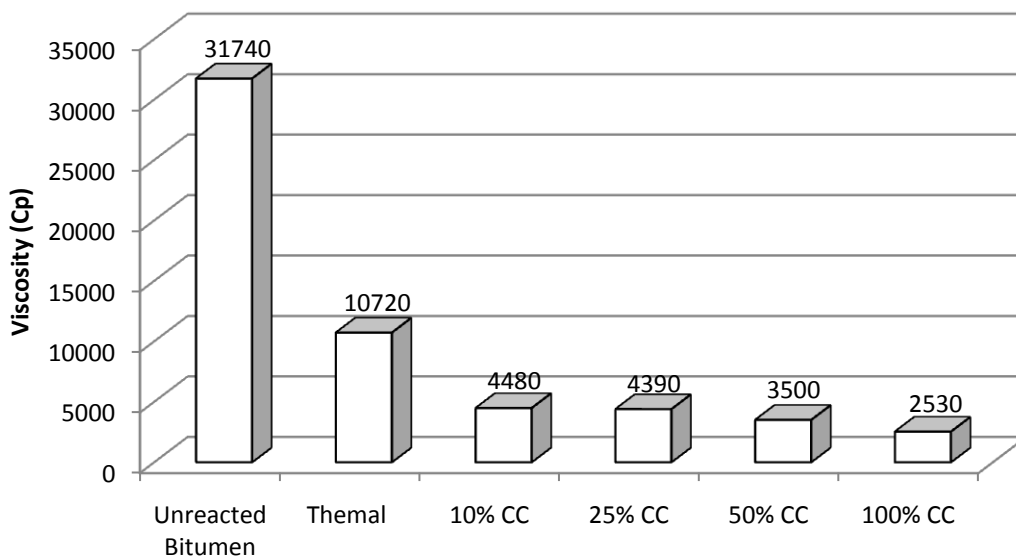


Figure 3-11 – Viscosity of pre-extracted bitumen as a function of varying levels of catalyst performed on bitumen at 400 °C ^[31].

At 400 °C thermal cracking has a modest effect, reducing the viscosity to one-third of the initial raw bitumen viscosity. The catalyst has a greater effect, reducing the viscosity to less than one seventh of the raw bitumen at only 10 % catalyst loading. The reduction in viscosity is minimal when the catalyst loading increases from 10 % to 25 %. A more substantial difference is seen at 50% and 100% loading where the viscosity drops 1000 and 2000 centipoises respectively. However, the better return for the amount of catalyst loading is observed at 10 % catalyst loaded reaction. Based on this observation we decided to perform the runs in the bitumen reactions at 10% catalyst loading.

Time Dependence Study

The effect of time on the cracking ability of the catalyst results are shown below in Figure 3-12.

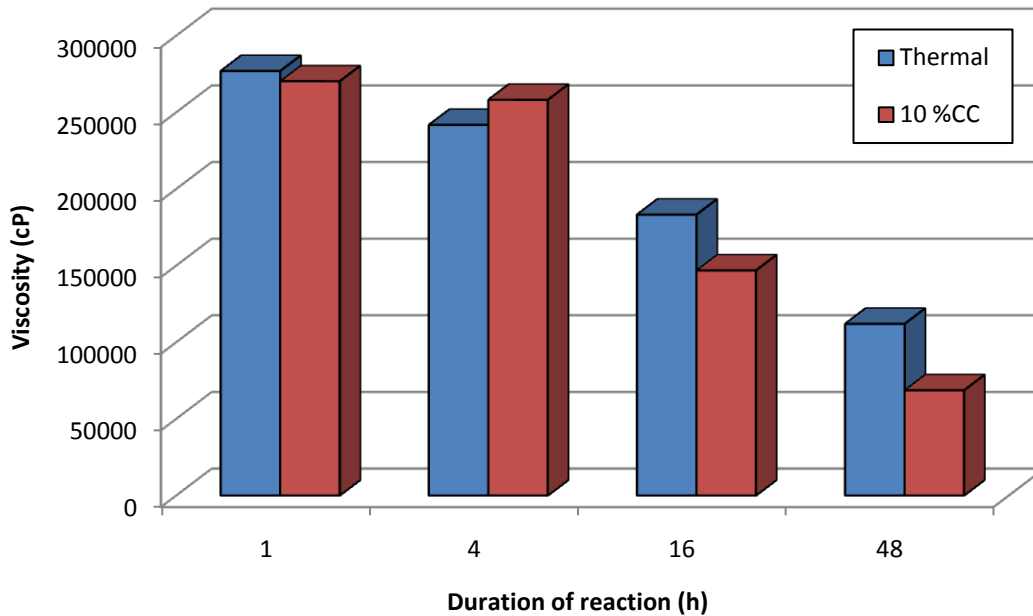


Figure 3-12 – Bitumen product viscosities for thermal and 10 % calcium chabazite catalyst loading reactions at 300 °C as a function of varying reaction times.

Overall it can be seen that the calcium chabazite (CC) runs generally outperform the thermal runs in lowering the viscosity. There is a small anomaly during the 4 hour runs where the catalyzed reaction undergoes a negligible change during hours 2-4. This allowed the thermal run to catch up to the CC run, passing it by 17 thousand cP. This changed in the 16 hour run where the catalyst resumed outperforming the thermal run. At 48 hours, the products of the catalyzed reaction have a viscosity of 69000 cP, which is 60 % that of the equivalent thermal run and 25 % of the viscosity after its 1 hour run.

These tests were done to investigate the possibility of combining this upgrading method with other prolonged *in situ* operations, such as the SAGD process. The catalyst would function especially well in the start up phase of the SAGD process, a process that normally takes 2-4 months for the two well bores to break up the oil between them ^[32]. The addition of the natural zeolite catalyst could reduce the start up time dramatically, and possibly upgrade the oil during the production of the well.

Catalytic Effect and Reusability

To determine if the catalyst could be recovered and reused for cracking, two runs were performed (level 1) with either chabazite or silica as the reactant. Powdered silica was used as a thermal run control group. After the extraction, the silica and the chabazite were recovered and reused in a second reaction (level 2). The results are shown below in Figure 3-13.

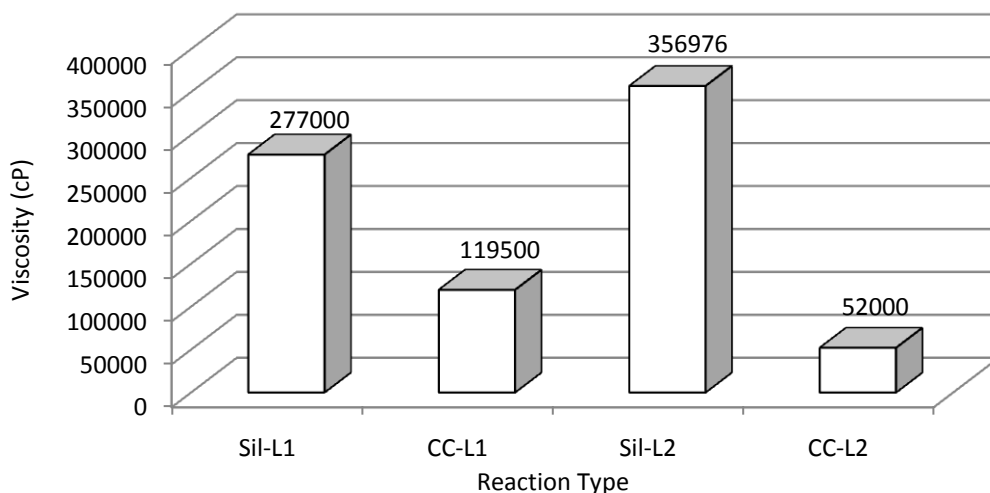


Figure 3-13 – Reusability runs with 10 % reactant loading at 300 °C across 2 runs as a function of viscosity.

As expected, the natural zeolite cracks the bitumen better than the silica in both the first and the second reactions. From the first level to the second level, the viscosity of the silica goes up, while the calcium chabazite goes down. Both these effects could be attributed to coke forming on the catalyst during the initial reaction. In the case of the silica the coke forming on the surface of the catalyst might interfere with the cracking of the heavy products and hence the viscosity is higher in the second reaction. In the case of the CC catalyst, it could be that the coke deposited on its surface interferes with the cracking of the lighter fraction, preventing the medium fractions from becoming light fractions that are lost to the vapour phase. This could also explain the lack of difference between the 1 and 4 hour reactions, of the time dependence experiments. The reason could be that the reaction is cracking at an equal rate for both the heavy and the light fractions and

so no headway is gained in terms of viscosity reduction after the initial drop.

After the 4 hour run, the small pores that only the lighter fractions could enter, were blocked by coke, meaning that no further valuable middle fractions could be lost.

These results are important for the potential use of natural zeolite in prolonged *in situ* operations such as SAGD. The zeolite catalyst would not be deactivated quickly and could continue to crack the heavy fractions over an extended period of time.

Chapter 4. Conclusion

Calcium chabazite was used in bench scale reactions as a catalyst to improve both the yield and quality of extracted bitumen at low temperatures and ideally accomplish it in one process. Natural zeolites substantially increased the industrially desired maltenes yield, while limiting the production of unwanted products such as gas and coke at a low reaction temperature of 300 °C. The maltenes yield increased at the expense of the C5 asphaltenes content. The data also revealed a trend of increasing cracking with higher temperature, 350 °C, and higher catalyst loading. Zeolites' efficacy at cracking carries with it the risk of overcracking as evidenced by large gas and coke yields at higher temperatures. The ideal operating conditions were determined to be a high catalyst loading at lower reaction temperature, taking advantage of the increased cracking under high loading conditions but avoiding overcracking that happens at high temperature. At the established operating conditions we observed increased maltenes yield, high C5 asphaltenes conversion and low coke and gas production.

In terms of product quality, reactions at the higher temperatures performed better as shown by both the SARA fractionation and the viscosity measurements. The high temperature, high catalyst loading conditions improved the quality of the bitumen products the most. However, even at lower temperature, the catalyst had substantial upgrading effects on the bitumen.

An additional benefit of using a natural zeolite catalyzed cracking process is that upgrading and cracking can happen at the same time. This will reduce the capital cost reduction by eliminating one process step while making the handling of the bitumen much easier, earlier in the process compared to the current industrial method. Another significant benefit is the environmental aspect as the natural zeolite-based process uses 1/10th of the water of the current process. This might have far reaching implications considering the amount of negative publicity the tailings ponds have created for the oilsands industry and Alberta itself.

To determine the practicality of this process, a comparison of energy balances was conducted between the proposed process and a simplified model of the current industrial process. It was found that the proposed process is more energy intensive than the current method. A separate energy balance was done to investigate if using zeolite solely as an upgrading catalyst on pre extracted bitumen would be more energy efficient. It was found that comparing a zeolite upgrading process to conventional primary upgrading, the zeolitic process required less energy.

Further investigation was performed to determine the extent of upgrading benefits. The results demonstrate that the untreated calcium chabazite could be used as an upgrading catalyst on extracted bitumen, lowering its viscosity substantially compared to the thermal treatment, especially at prolonged reaction times. It was

also confirmed that the natural zeolite was acting as a catalyst. The results have interesting implications because natural zeolites could potentially be used in *in situ* processing methods, such as SAGD, to upgrade and aid in the collection of the bitumen.

Future Work

One area that could be further investigated is the possibility of decreasing the energy consumption of the stirred oilsands reactions. More exploratory studies could be conducted to determine if the reactions could be performed at even lower temperatures and if the solvent to bitumen ratio in the extraction step could be lowered. Another avenue of investigation could be the use of heat exchangers to save the large amount of energy expended in the proposed process. These areas show promise as they may contribute to developing an economical and environmentally friendly natural zeolite based process for stirred oilsands reactions.

A second area that requires more attention is the possibility of including zeolite in SAGD and other *in situ* operations. This area could greatly improve the startup time for a SAGD well pair, as well as upgrade the bitumen while it is being extracted.

Chapter Five. Bibliography

- [1] O. Strausz, E. Lown, The chemistry of Alberta oil sands, bitumens and heavy oils, *Alberta energy research institute*, Canada, 2003, 17-19
- [2] K. Bukka, J. D. Miller, A. G. Obladt, Fractionation and Characterization of Utah Tar Sand Viscosity, *Energy & Fuels*, 1991, **5**, 333-340
- [3] G. Brons, J. Yu, Solvent Deasphalting Effects on Whole Cold Lake Bitumen, *Energy & Fuels*, 1995, **9**, 641-647
- [4] Alberta Department of Energy,
<http://www.energy.alberta.ca/OilSands/791.asp>, accessed January 2011
- [5] Alberta Energy, <http://www.energy.gov.ab.ca/OurBusiness/oilsands.asp>, accessed January 2011
- [6] Alberta's Energy Reserves 2009 and Supply/Demand Outlook 2010-2019,
http://www.ercb.ca/portal/server.pt/gateway/PTARGS_0_0_308_265_0_43/http%3BercbContent/publishedcontent/publish/ercb_home/publications_catalogue/publications_available/serial_publications/st98.aspx, accessed January, 2011
- [7] Guntis Moritis, Alberta bitumen output to triple in next 10 years, *Oil & Gas Journal*, Sep 25, 2006; **104**, 36
- [8] R. Marsh, F. Hein, Canada's extra-heavy (bitumen) and heavy oil resources, reserves and development, *J. Can. Pet. Tech*, 2008, **47** (5), 7-11
- [9] M. Gray, J. Masliyah, Extraction and Upgrading of Oilsands Bitumen, course notes, Feb 2002
- [10] U.G. Romanova, H.W. Yarranton, L.L. Schramm, W.E. Shelfantook, Investigation of Oil Sands Froth Treatment, *Can. J. Chem. Eng.*, **82**, Aug 2004, 710-721
- [11] D. R. Gotawala, I. D. Gates, Stability of the edge of a SAGD steam chamber in a bitumen reservoir, *Chemical Engineering Science*, **66**, 2011, 1802–1809

- [12] D.L. Chow, T.N. Nasr, R.S. Chow, R.P. Sawatzky, Recovery techniques for Canada's heavy oil and bitumen resources, *J. Can. Pet. Tech.*, 2008, **47** (5), 12-17
- [13] H.Z. Ha, P. Koppel, Accurately predict viscosity of Syncrude blends, *Hydrocarbon Processing*, July 2008, 87-92
- [14] G.A. Nunez, H.J. Rivas, D.D. Joseph, Drive to produce heavy crude prompts variety of transportation methods, *Oil & Gas Journal*, Oct 26, 1998, **96**, 43
- [15] A. Dyer, Introduction to zeolite molecular sieves, Bath press ltd., Great Britian, 1988, 1-4 & 117-135
- [16] C. Baerlocher, L. B. McCusker, D. H. Olson, Atlas of Zeolite Framework Types 6th ed., Elsevier B.V., 2007
- [17] J. Weitkamp, Michael Hunger, Acid and base catalysis on zeolites, In *Introduction to zeolite science and practice 3rd ed.*, J. Cejka, H. van Bekkum, A. Corma, F. Schuth, Ed., Elsevier, 2007, 1-13
- [18] S. R. Stoyanov, S. Gusarov, S. M. Kuznicki, A. Kovalenko, Theoretical Modeling of Zeolite Nanoparticle Surface Acidity for Heavy Oil Upgrading, *J. Phys. Chem. C*, 2008, **112**, 6794-6810
- [19] M. Rigutto, Cracking and Hydrocracking, In *Zeolites and catalysis: synthesis, reactions and applications*, J. Cejka, A. Corma S. Zones, Ed., Wiley-VCH, 2010, 547-585
- [20] T. Maesen, The zeolite scene – an overview. In *Introduction to zeolite science and practice 3rd revised edition*, J. Cejka, H. van Bekkum, A. Corma, F. Schuth, Ed., Elsevier, 2007, 1-13
- [21] L.A. Pine, P.J. Maher, W.A. Wachter, Prediction of cracking catalyst behaviour by a zeolite unit cell size model, *J. Cat.*, 1984, **85**, 466-476
- [22] M. Occelli, Recent trends in fluid catalytic cracking technology, *ACS symposium series*, 1988, **375**, 1-16
- [23] M.C. Galiano, U.A. Sedran, Light Alkene Selectivity on Y Zeolite FCC Catalysts, *Ind. Eng. Chem. Res.*, 1997, **36**, 4207-4211
- [24] R. Sadeghbeigi, Fluid catalytic cracking handbook 2nd ed., Elsevier Gulf, 2000

- [25] A.S.M. Junaid, H. Yin, A. Koenig, P. Swenson, J. Chowdhury, G. Burland, W.C. McCaffrey, S.M. Kuznicki, Natural zeolite catalyzed cracking-assisted light hydrocarbon extraction of bitumen from Athabasca oilsands, *Applied catalysis A*, 2009, **354**(1-2), 44-49
- [26] S.M. Kuznicki, W.C. McCaffrey, J. Bian, E. Wangen, A. Koenig, C.C.H. Lin, Natural zeolite bitumen cracking and upgrading, *Microporous and Mesoporous Materials*, 2007, **105**, 268–272
- [27] ASTM standard, D 95, 2005 (2010), Standard Test Method for Water in Petroleum Products and Bituminous Materials by Distillation, ASTM International
- [28] ASTM standard, D 2007, 2003 (2008), Standard Test Method for Characteristic Groups in Rubber Extender and Processing Oils and Other Petroleum-Derived Oils by the Clay-Gel Absorption Chromatographic Method, ASTM International
- [29] J. Masliyah, Fundamentals of Oils Sands Extraction, Course Notes, 2011
- [30] A.S.M. Junaid, M. Rahman, H. Yin, W.C. McCaffrey, S.M. Kuznicki, Natural Zeolites for Oilsands Bitumen Cracking: Structure and Acidity, *Microporous and Mesoporous Materials*, 2011
- [31] A.S.M. Junaid, W. Wang, C. Street, M. Rahman, M. Gersbach, S. Zhou, W. McCaffrey, S. M. Kuznicki, Viscosity Reduction and Upgrading of Athabasca Oilsands Bitumen by Natural Zeolite Cracking, World Academy of Science, Engineering and Technology, 2010, **69**
- [32] C. Chakrabarty J.-P. Fossey, G. Renard, C. Gadelle, SAGD Process in the East Senlac Field: From Reservoir Characterization to Field Application, *7th UNITAR International Conference on Heavy Crude and Tar Sands*, 1998, **192**

Chapter Six. Appendix

Copyrighted Materials Permissions:

[11]

Your order details and publisher terms and conditions are available by clicking the link below:

http://s100.copyright.com/CustomerAdmin/PLF.jsp?IID=2011041_1303413687400

Order Details

Licensee: Christopher A Street

License Date: Apr 21, 2011

License Number: 2653790639400

Publication: Chemical Engineering Science

Title: Stability of the edge of a SAGD steam chamber in a bitumen reservoir

Type Of Use: reuse in a thesis/dissertation

Total: 0.00 USD

[16]

Your order details and publisher terms and conditions are available by clicking the link below:

http://s100.copyright.com/CustomerAdmin/PLF.jsp?IID=2011041_1303410754900

Order Details

Licensee: Christopher A Street

License Date: Apr 21, 2011

License Number: 2653770730900

Publication: Elsevier Books

Title: Atlas of Zeolite Framework Types (Sixth Edition)

Type Of Use: reuse in a thesis/dissertation

Total: 0.00 USD